

THE FLUIDISED BED COMBUSTION CHARACTERISTICS OF SOME
INFERIOR QUALITY SOUTH AFRICAN COALS.

Andre Pieter Hamman

THE FLUIDISED BED COMBUSTION CHARACTERISTICS OF SOME
INFERIOR QUALITY SOUTH AFRICAN COALS.

Andre Pieter Hanman

A dissertation submitted to the Faculty of Engineering,
University of the Witwatersrand, Johannesburg, in fulfilment
of the requirements for the degree of Master of Science in
Engineering.

Johannesburg, 1985

I declare that this dissertation is my own, unaided work. It is being submitted for the Master of Science in Engineering in the University of the Witwatersrand, Johannesburg. It has not been submitted before for any degree or examination in any other University.

A. Hamman

29th day of March 1985

ABSTRACT

South Africa is presently faced with the problem of an immense under utilization of inferior quality coal types. An experimental program, employing a specially designed laboratory scale fluidized bed, has been undertaken to determine the fluidized bed combustion characteristics of two low grade South African coals namely, Tavistock Duff and Rietspruit Discard coals. The significance of these particular coals, is that they are to be used as the primary feedstocks for the National fluidized bed combustion demonstration boiler. The Rietspruit discard coal has a considerably higher percentage ash content than the Tavistock duff coal, which is regarded as low grade only by virtue of its poor size distribution.

A laboratory scale fluidized bed, having an internal diameter of 76mm, was constructed to facilitate the batch wise combustion of the two coal types. The experimental programme involved the burning of coal samples of known particle size and carbon mass under preset operating conditions. The combustion experiments provided the basis for the development of relevant combustion models, as well as providing a greater insight into the combustion behaviour of these two types of coal.

The derived combustion models are based on the two-phase theory of fluidization and incorporate both film diffusional and kinetic resistances. The investigation has shown that the combustion of *Rietspruit Discard* follows the "shrinking core" mode of reaction, while the combustion of *Tavistock Duff* follows the "shrinking particle" mode of reaction. The mathematical models were found to satisfactorily represent the combustion behaviour of the particular coals investigated. The findings of this research work will be incorporated into the NFBC research programme.

In Monasterio Anne

ACKNOWLEDGEMENTS

I am most grateful to the National Institute for Coal Research, whose facilities made this project possible and to Dr. C.M. Eleftheriades for his invaluable inspiration and guidance throughout the duration of this investigation. Furthermore, I would like to thank Prof. A. Bryson, Prof. M. R. Judd and Prof. D. Glasser for their assistance.

<u>CONTENTS</u>	page
DECLARATION	ii
ABSTRACT	iii
ACKNOWLEDGEMENTS	iv
CONTENTS	v
LIST OF FIGURES	vii
LIST OF TABLES	ix
LIST OF SYMBOLS	x
1. INTRODUCTION	1
2. LITERATURE REVIEW ON ASPECTS OF THE FLUIDISED BED COMBUSTION OF COAL	2
2.1 Combustion of volatiles	2
2.2 Combustion of char	4
2.2.1 char combustion reaction resistances	4
2.2.2 char combustion reaction mechanism	6
2.2.3 char combustion models	10
3. THEORY	14
3.1 Two phase theory of fluidization	15
3.2 Coal devolatilization	18
3.3 Combustion of char	19
3.3.1 shrinking particle combustion model	20
3.3.2 shrinking core combustion model	25
4. ASSUMPTIONS AND CALCULATION PROCEDURE	27
4.1 Calculation assumptions	27
4.2 Regression algorithm to determine the model parameters	30
4.3 Prediction of carbon dioxide in the flue gas	31

5. EXPERIMENTAL PROCEDURE	32
6. ANALYSIS OF THE EXPERIMENTAL COMBUSTION RESULTS	36
6.1 Qualitative description	37
6.1.1 the effect of the fluidized bed operating conditions on combustion	37
6.1.2 the effect of the coal characteristics on combustion	40
6.2 The mathematical description of the combustion data	45
6.2.1 analysis of Tavistock duff coal	45
6.2.2 analysis of Rietspruit discard coal	68
7. EVALUATION OF THEORETICAL APPROACH	66
8. CONCLUSION	75
9. REFERENCES	77
APPENDICES	
APPENDIX A - Experimental burnout time data	74
APPENDIX B - Program MOD and TRACE	83
APPENDIX C - Effect of variation of particle surface temperature on combustion behaviour.	86
APPENDIX D - Elutriation data for Tavistock coal	87
APPENDIX E - Bed temperature profile for a series of Tavistock coal combustion experiments	88
APPENDIX F - Dimensioned fluidized bed reactor drawings	98

<u>LIST OF FIGURES</u>	page
2.1 Two-film reaction mechanism.	8
2.2 Direct oxidation reaction mechanism.	8
3.1 Fluidized bed reactor according to the two phase theory	16
5.1 Fluidized bed reactor system	33
6.1 Burnout time versus bed temperature.	38
6.2 Effect of temperature on the combustion of Tavistock Duff.	39
6.3 Tavistock burnout time versus fluidizing gas velocity.	41
6.4 Burnout time versus particle diameter.	41
6.5 Burnout time versus particle diameter squared.	41
6.6 Effect of particle diameter on the combustion of Tavistock Duff.	42
6.7 Comparison of carbon dioxide traces of Rietspruit Discard and Tavistock Duff.	42
6.8 Tavistock burnout time versus mass of carbon charge $T_b=715\text{ }^\circ\text{C}$ $R_t=4$ $\tau_v=180$ s	51
6.9 Tavistock burnout time versus mass of carbon charge $T_b=715\text{ }^\circ\text{C}$ $R_t=6$ $\tau_v=180$ s	51
6.10 Tavistock burnout time versus mass of carbon charge $T_b=715\text{ }^\circ\text{C}$ $R_t=8$ $\tau_v=180$ s	52
6.11 Tavistock burnout time versus mass of carbon charge $T_b=715\text{ }^\circ\text{C}$ $R_t=4$ $\tau_v=0$	52
6.12 Tavistock burnout time versus mass of carbon charge $T_b=715\text{ }^\circ\text{C}$ $R_t=6$ $\tau_v=0$	53
6.13 Tavistock burnout time versus mass of carbon charge $T_b=715\text{ }^\circ\text{C}$ $R_t=8$ $\tau_v=0$	53
6.14 Tavistock burnout time versus mass of carbon charge $T_b=848\text{ }^\circ\text{C}$ $R_t=6$ $\tau_v=180$ s	54
6.15 Tavistock burnout time versus mass of carbon charge $T_b=848\text{ }^\circ\text{C}$ $R_t=8$ $\tau_v=0$	54
6.16 Comparison of model predictions $\tau_v=180$ s $T_b=715\text{ }^\circ\text{C}$	55
6.17 Comparison of model predictions $\tau_v=0$ $T_b=715\text{ }^\circ\text{C}$	55
6.18 Tavistock carbon dioxide trace prediction $T_b=715\text{ }^\circ\text{C}$ $R_t=4$ $D_i=1.09$	56
6.19 Tavistock carbon dioxide trace prediction $T_b=715\text{ }^\circ\text{C}$ $R_t=4$ $D_i=3.08$	56

6.20 Tavistock carbon dioxide trace prediction $T_b=715$ °C $R_t=4$ $D_i=4.5$	57
6.21 Tavistock carbon dioxide trace prediction $T_b=715$ °C $R_t=8$ $D_i=1.09$	57
6.22 Tavistock carbon dioxide trace prediction $T_b=715$ °C $R_t=8$ $D_i=3.08$	58
6.23 Tavistock carbon dioxide trace prediction $T_b=715$ °C $R_t=8$ $D_i=4.5$	58
6.24 Rate constant versus particle surface temperature.	59
6.25 Burnout time versus mass of carbon charge $T_b=715$ °C $R_t=6$ $\tau_0=9D_i^{1.02}$	63
6.26 Comparison of Rietspruit carbon dioxide trace predictions $T_b=715$ °C $\tau_0=9L_i^{1.02}$ $D_i=4.5$	63
6.27 Rietspruit carbon dioxide trace prediction $T_b=715$ °C $R_t=6$ $D_i=4.5$	64
6.28 Rietspruit carbon dioxide trace predictions $T_b=715$ °C $R_t=6$ $D_i=3.08$	64
6.29 Oxygen fraction versus dimensionless rate constant	65
7.1 Dependence of overall resistance to combustion on particle size. (Ross & Davidson 1981)	69
7.2 Overall combustion resistance versus particle diameter.	69
7.3 Prediction of carbon dioxide trace $T_b=715$ °C $R_t=4$.	74
E.1 Temperature profiles for a typical series of Tavistock combustion trials.	89
F.1 Sectioned side view of fluidized bed reactor.	91
F.2 Top view of distributor plate.	92
F.3 Sectioned side view of distributor plate	92

<u>LIST OF TABLES</u>	page
4.1 Values of the physical constants used in the experimental data regression.	29
5.1 Operating conditions.	34
5.2 Coal characteristics.	34
5.3 Coal particle diameters.	35
6.1 Linear regression of τ versus M_c plots for Tavistock at 715 °C.	46
6.2 Regression results for combustion of Tavistock Duff at 715 °C.	47
6.3 Regression results for combustion of Tavistock Duff at 840 °C.	48
6.4 Regression results for combustion of Rietspruit Discard at 715 °C.	68
7.1 The Sherwood number and rate constant values evaluated for Tavistock coal at 715 °C and with $\tau_v=180 \mu\text{s}$.	68
D.1 Elutriation data for the combustion of Tavistock Duff coal at 715 °C and $U=0.198 \text{ m/s}$.	87

LIST OF SYMBOLS

- a - constant in devolatilization time expression (s/mm)
- A - lumped flowrate parameter (m^3/s)
- A_r - reactor cross-sectional area (m^2)
- b - constant defining combustion mechanism
- $C_{B,C1}$ - combustion model coefficients (s)
- $C_{2,C3}$ - combustion model coefficients (s)
- C - concentration ($Kmol/m^3$)
- C' - ratio of inlet concentration to outlet concentration
- C_{bh} - bubble phase oxygen concentration at a height H from the distributor ($Kmol/m^3$)
- C_h - outlet oxygen concentration ($Kmol/m^3$)
- C_o - inlet oxygen concentration ($Kmol/m^3$)
- C_p - particulate phase oxygen concentration ($Kmol/m^3$)
- C_s - particle surface oxygen concentration ($Kmol/m^3$)
- D - particle diameter (m)
- D_i - initial particle diameter (m)
- D_e - ash layer diffusion coefficient (m^2/s)
- D_g - gas phase diffusion coefficient (m^2/s)
- F - variation factor in equation (E.7.1)
- f_c - fraction of fixed carbon in coal
- H - expanded fluidized bed height (m)
- H_o - bed height at incipient fluidization (m)
- k - first order reaction rate constant (m/s)
- k' - dimensionless rate constant
- K_g - mass transfer coefficient (m/s)
- K_c - surface reaction rate constant (m/s)
- K - overall rate constant (m/s)
- M - mass of coal sample (kg)
- M_c - mass of carbon charge (kg)
- M_o - mass flowrate of inlet air (kg/s)
- m - constant in generalized burnout time-diameter expression
- N - number of char particles
- n - flux of oxygen to a particle ($Kmol/s$)
- q - volume flowrate in and out of bubble (m^3/s)

R	- reaction zone radius (m)
R_C	- carbon combustion rate (kmol/s)
Re	- Reynolds number
R_g	- universal gas constant (kJ/kmol.K)
R_t	- 14E Rotameter float height (cm)
S	- sum of squared errors in regression algorithm
Sc	- Schmidt number
Sh	- Sherwood number
t	- time (s)
t_c	- time relevant to char combustion (s)
T_b	- bed temperature (K)
T_p	- particle surface temperature (K)
U	- gas velocity through reactor (m/s)
U_b	- bubble velocity (m/s)
U_o	- minimum fluidizing velocity (m/s)
V	- bubble volume (m ³)
u	- constant in devolatilization time expression
X	- cross-flow factor
x	- particle diameter ratio
y	- variable Sh model coefficient
z	- variable Sh model coefficient

Greek symbols

ρ_c	- char density (kg/m ³)
T_b	- burnout time of coal sample (s)
T_c	- burnout time of char particles (s)
T_j	- interphase oxygen transfer burnout time (s)
T_s	- particle size dependent burnout time (s)
T_v	- devolatilization time (s)
ω_j	- regression algorithm variable (s)
ν_j	- regression algorithm variable (m)
β	- velocity ratio parameter
γ, α	- reaction mechanism constants

Abbreviations

CSTR	- Continuous Stirred Tank Reactor.
NFBC	- National Fluidized Bed Combustion demonstration boiler.
SCM	- Shrinking Core Model.
SPM	- Shrinking Particle Model.

1. INTRODUCTION

South Africa is presently faced with the problem of an immense under utilization, and consequently a high rate of accumulation, of inferior quality coal types. A national research program has been established and funded by the government to investigate the combustion of these coal types in a fluidized bed combustor.

In order to predict the performance of a fluidized bed combustor it is essential to have an understanding (preferably a mathematical model) of the coal's combustion behaviour. To date limited research work has been done to establish the fluidized bed combustion characteristics of South African coals. For this reason an experimental program, employing a specially designed laboratory scale fluidized bed, has been undertaken to determine the combustion characteristics of two low grade South African coals namely, Tavistock Duff and Rietspruit Discard coals. The significance of these particular coals, is that they are to be used as the primary feedstocks for the National Fluidized Bed Combustion (NFBC) demonstration boiler. The Rietspruit coal has a considerably higher percentage ash content than the Tavistock coal, which is regarded as low grade only by virtue of its poor size distribution.

The objectives of this research work are to investigate experimentally the fluidized bed combustion behaviour of the Rietspruit Discard and Tavistock Duff coals and develop relevant combustion models. The experimental combustion data will enable one to critically assess the validity of the proposed models and their associated assumptions.

This thesis incorporates an overview of the relevant theory, a presentation and analysis of the experimental combustion results and finally a discussion of the applicability of the proposed combustion models.

2. LITERATURE REVIEW ON ASPECTS OF THE FLUIDIZED BED COMBUSTION OF COAL.

The fluidized bed combustion of coal is a complex process involving the interaction of chemical reactions with heat and mass transfer effects as well as the hydrodynamic characteristics of the fluidized bed.

Coal particles dropped into a hot fluidized bed will rapidly lose their volatile components which burn as a diffusion flame in the particle surroundings. During the devolatilization process the coal particles are at a temperature lower than the bed temperature and appear black against the glowing inert bed material. The combustion of the fixed carbon content of the residual material, ie char, proceeds after the devolatilization process. The char particles move freely throughout the bed and their surface temperature possibly exceeds the temperature of the bed inert material. The char combustion continues until a critical size is reached, whereupon the particles are carried into the freeboard region and eventually out of the reactor.

Coal combustion consists of two distinct processes, namely the devolatilization process and the char combustion process. The present understanding of these two processes is discussed in depth below.

2.1 COMBUSTION OF VOLATILES.

The major part of previous research work on coal combustion has concentrated on the combustion of char particles. The evolution of volatiles from coal particles is extremely complex. The rate of release of volatiles depends upon the heat transfer characteristics and temperature of the environment, the physical structure of the coal and the nature of the volatile content of the coal. The process is

complicated further if the volatiles are considered to be released into an oxidising atmosphere. The combustion of the volatiles involves a series of homogenous and heterogenous reactions. The numerous chemical reactions yield quantities of the oxides of nitrogen, sulfur, hydrogen and carbon. The volatile materials burn as a diffusion flame which surrounds the coal particle. During this period the coal particles are at a lower temperature than the bed temperature, (Yates, 1983), since the coal particles appear as black spots against the glowing inert bed material.

The emission of volatiles from coal particles in a fluidized bed has previously been assumed to occur instantaneously (Avedesian & Davidson (1975), Saxena & Turek (1980)). It is generally accepted that the total duration of the devolatilization process is only a small fraction of the total burning time of the coal particle. The bench work of Pillai, (1981) showed that the duration of the devolatilization process was significant and the assumption of instantaneous release of volatiles was incorrect.

Pillai, (1981) measured the devolatilization times for twelve different coal types in a fluidized bed combustor. The investigation examined a range of particle sizes (258µm - 8mm), bed temperatures (775-1010 °C) and coal sample masses (1-5g). The devolatilization times were measured visually as the time from the establishment of the volatiles combustion flame to the time at which this flame was extinguished. Pillai found that the coal batch size had only a weak effect on the measured devolatilization times. The following power law relationship was found to adequately describe the devolatilization times of the twelve coal types investigated :

$$T_v = a D_i^u$$

2.2 COMBUSTION OF CHAR.

To date considerable research work has been conducted to establish the nature of char combustion in a fluidized bed. Char combustion may be considered to comprise of two facets, namely the prevailing reaction mechanism and the limiting combustion resistances. The combination of these two facets provides the foundation for a combustion model. A review of the present understanding is given below.

2.2.1 Char combustion reaction resistances.

The combustion of char in a fluidized bed is generally thought to occur in a shrinking particle mode of reaction. It is believed that the scouring action present in a fluidized bed removes any ash layer that is formed and thus the fixed carbon is continuously exposed to the oxidising gas environment. However, for high ash content coals, the shrinking core mode of reaction is more appropriate (Pillar, 1981). The overall combustion resistance, which controls the rate of the combustion of char, is the summation of a number of resistances acting in series. The resistances are generally identified as follows :

- 1) a convective mass transfer resistance which represents the transfer of oxygen from the bubble phase to the particulate phase in the fluidized bed.
- 2) a film diffusion resistance which represents the transfer of oxygen from the particulate phase to the surface of the char particle.
- 3) an ash layer diffusion resistance which typically applies only to high ash content coals and which represents the diffusion of oxygen through the ash layer surrounding the char particle and
- 4) a chemical reaction resistance which represents the kinetic resistance of the surface combustion reactions.

The fluidized bed hydrodynamic model, employed in the description of the combustion process, accounts for the convective mass transfer resistance. The two-phase theory of fluidization has been successfully used to describe the mass transfer between the bubble and particulate phases (Avedesian & Davidson (1973), Gibbs (1975), Ross & Davidson (1981)).

Pioneering research work on the combustion of char accounted only for the film diffusional resistance, since the chemical reactions were considered to proceed relatively fast (Avedesian & Davidson 1973, Chen & Saxena 1977, Basu Broughton & Elliot 1975). The assumption that the chemical kinetics have no effect on the combustion rate has been questioned (Tomczek 1979, Pillai 1980) and consequently a fair amount of research has been conducted to establish the importance of the chemical kinetics. Chakraborty & Howard (1981) performed a series of batch-wise combustion experiments in a fluidized bed reactor using the char of a high volatile content bituminous coal. Their results indicated that at a bed temperature of 1073 K the kinetic resistance strongly influences the char combustion rate, whereas at a bed temperature of 1173 K the transfer of oxygen to the particle surface became the limiting resistance.

Pillai (1980) examined the combustion characteristics of several different coal types and generally found that the char types did not behave identically under the same conditions. A summary of the observed peculiarities of some selected coal types is presented below.

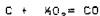
- The combustion of Texas lignite, at both the bed temperatures of 775 °C and 1010 °C, was found to exhibit a shrinking particle mode of reaction, which was entirely controlled by the film diffusion resistance.
- The combustion of Lohberg, a German bituminous coal, was strongly influenced by the chemical kinetic resistance over the whole temperature range investigated.

- The combustion of Agrina, an Irish high-ash coal of low reactivity, exhibited the shrinking core mode of reaction. At 775 °C the combustion rate was strongly controlled by the Kinetic resistance. The ash diffusion resistance was found to be limiting at 1010 °C.
- Glen Brook, an Ohio bituminous coal, displayed a shrinking particle mode of reaction. The Kinetic resistance was found to be limiting at 775 °C. At 1010 °C the combustion was influenced by a combination of the film diffusion and Kinetic resistances, with the film diffusion resistance been the dominant resistance.

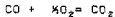
The temperature dependance of the limiting resistances follow the generally accepted trend (Levenspiel, 1972), i.e. at low temperatures the rate of combustion is limited by the chemical kinetics and as the temperature increases the film diffusion resistance becomes increasingly dominant. It is apparent from the above discussion that the relative roles of the combustion resistances are strongly dependant on both the reactor conditions and the nature of the coal.

2.2.2 Char combustion reaction mechanism.

The combustion of char occurs via a series of surface and gas-phase reactions. The important surface reactions are as follows (Field 1967)



The gas-phase reaction is the following :



The extent and location of these reactions depends upon the coal type, particle diameters, particle temperatures, etc. Several combustion mechanisms, employing the above mentioned reactions, have been proposed. Two notable mechanisms are reviewed below, viz. the two-film reaction mechanism and the direct oxidation reaction mechanism.

Hougen & Watson (1947) considered the char combustion to proceed in the following fashion. Initially oxygen diffuses to the char surface and reacts with the fixed carbon to produce CO. The CO diffuses towards the interstitial gas stream where it reacts with the incoming oxygen to produce carbon dioxide. One half of the carbon dioxide diffuses back to the char particle surface where it is reduced to CO. The other half of the carbon dioxide diffuses into the main gas stream. This reaction mechanism is known as the two-film model, (see figure 2.1). Avedesian & Davidson (1973) adopted the above mechanism in their pioneering research work and considered the gas phase oxidation of carbon monoxide to occur as a diffusion flame in a thin reaction zone which surrounded the char particles. Their analysis of the concentration profiles which surround the char particles showed that the reaction zone thickness was half the diameter of the particle. This dimension is based on the assumption of a zero particulate phase carbon dioxide concentration. Campbell & Davidson (1975) considered the case of a finite particulate phase carbon dioxide concentration and derived an expression for the reaction zone radius (R), namely :

$$R = D(C_0 + C_p)/2C_p \quad \text{-----} \quad (E.2.2)$$

According to equation (E.2.2), the reaction zone radius will become large for small concentrations of particulate phase oxygen. If this were to occur a large amount of the "reaction energy" would be dissipated by the inert bed material and consequently little energy would be available to sustain the endothermic surface reaction. On this basis Campbell & Davidson (1975) inferred that the reaction zone

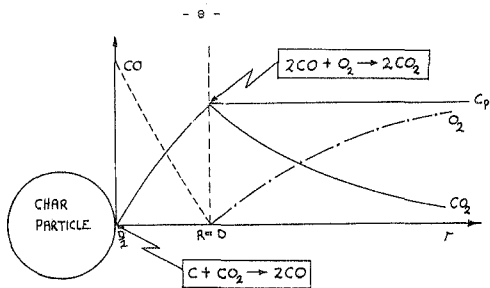


Figure 2.1 Two-film reaction mechanism.

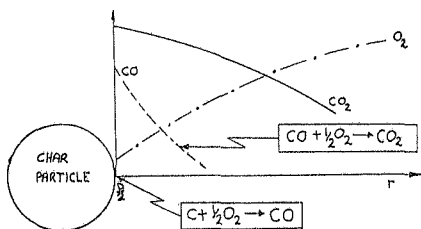


Figure 2.2 Direct oxidation reaction mechanism.

radius is restricted by the heat transfer characteristics of the combustion environment. They assumed a generalized expression for the radius of the reaction zone, viz:

$$R = b D/2 \quad \text{-----} \quad \text{(E.2.3)}$$

The value of b may be seen as an indication of the location of the CO combustion reaction. For $b=1$ the CO combustion occurs at the surface of the particle which results in the complete oxidation of carbon to carbon dioxide at the char surface. For $b=2$, which is the case considered by Avedesian & Davidson (1973), the CO combustion occurs in a reaction zone surrounding the particles.

The validity of the two-film reaction mechanism has been questioned by several researchers (Basu, Broughten & Elliot(1975), Borghi, Sarofim & Beer(1977), Ross & Davidson(1981)). It is felt that the Boudouard reaction (which is the surface reaction according to the two-film mechanism) does not occur to any appreciable extent under the typical fluidized bed operating conditions viz. bed temperature in the range 700-900 °C. The experimental findings of Golovina & Khaustovich (1962) have shown that the rate of the Boudouard reaction is too slow to account for the observed combustion rates.

Using experimentally derived temperatures and dimensions Basu et al performed an energy balance on a burning char particle to establish the nature of the surface reaction. Their calculations showed that there is little possibility of the endothermic Boudouard reaction occurring at the char surface. Basu et al assumed a reaction mechanism which visualizes the oxygen to diffuse to the char surface and react directly with the fixed carbon of the char to produce both carbon dioxide and carbon monoxide. The carbon monoxide is subsequently burnt in a reaction zone which surrounds the particle. This reaction mechanism has become known as the direct oxidation mechanism and is depicted in figure 2.2. The applicability of the direct oxidation model is supported further by the kinetic data of Field (1967) and

Arthur (1951) which shows that the Boudouard reaction is too slow to compete with the oxidation of carbon by oxygen. Ross & Davidson (1981) analyzed the combustion of char using both the direct oxidation and the two-film mechanisms. Their experimental data showed that the reduction of carbon dioxide to carbon monoxide on the char surface is negligible. In their interpretation of the direct oxidation mechanism, they considered the char surface reaction to produce only carbon monoxide. The oxidation of the carbon monoxide was assumed to occur either rapidly or at a slow rate. For the case of a rapid CO combustion reaction, the CO is consumed very close to the char surface, which results in an effective overall oxidation of carbon to carbon dioxide at the surface. For the case of relatively slow CO oxidation rates, the CO is consumed in the surroundings of the burning particles. The above interpretation of the direct oxidation mechanism is very similar to the modified two-film mechanism of Campbell & Davidson (1975). In fact if the CO oxidation reaction is considered to proceed rapidly and the value of b in equation (E.2.3) is taken as 1, then the two mechanisms are identical, viz. the effective direct oxidation of carbon to carbon dioxide at the surface of the char particles.

2.2.3 Char combustion models.

The combustion model used by Arvedsson & Davidson (1973) is based on the two phase theory of fluidization and the two film reaction mechanism. The film diffusion resistance was considered to be the limiting resistance as the chemical reactions were assumed to proceed rapidly. The expression they obtained for the char burnout time as a function of the initial particle diameter is given by equation (E.2.4).

$$\tau_c = \frac{M_c}{12 C_o A_p (U - (U - U_o) \exp(-X))} + \frac{D_p^2 P_c}{96 Sh D_o C_o} \quad \text{--- (E.2.4)}$$

The initial diameter squared term in equation (E.2.4) represents the film diffusion resistance. The convective

mass transfer resistance is represented by the LHS term in equation (E.2.4). A consideration of the kinetic resistance would produce an additional term in initial diameter. The char burnout times, which were measured visually, were plotted against the square of the initial particle diameter, cf. equation (E.2.4). Based on the straight line plots obtained they concluded that the combustion process was indeed controlled by the film diffusion resistance.

It has been pointed out by Tomczek (1979) that the burnout time data of Avedesian et al would also produce acceptable straight line plots if plotted against the initial particle diameter. Straight line plots of this nature would indicate that the kinetic resistance was limiting.

The research work of Ross & Davidson (1981) considered the combustion of char particles in the temperature range of 1183 to 1173 K in order to establish the relative importance of film diffusion and reaction kinetics in determining the rate of combustion. They derived three combustion models, which were all based on the two phase theory of fluidization. Furthermore, all the models incorporated both the film diffusion and kinetic resistances. The models differed in their approach to the combustion reaction mechanism. The mechanisms considered were the two film reaction mechanism, the direct oxidation reaction mechanism assuming the CO reaction to proceed rapidly and the direct oxidation mechanism assuming the CO reaction to proceed slowly. The derived burnout time expressions were similar to equation (E.2.4), except for an additional kinetic resistance term which contained the surface reaction rate constant. Their theoretical analysis resulted in the following relation between the overall combustion resistance ($1/K$) and the parameters of the kinetic resistance (K_c) and the film diffusion resistance (Sh).

$$\frac{1}{K} = \gamma \frac{1}{K_c} + \frac{\alpha D}{Sh D_0} \quad \text{----- (E.2.5)}$$

γ and α are constants whose values depend on which reaction mechanism is assumed to occur. The experimental

mass transfer resistance is represented by the LHS term in equation (E.2.4). A consideration of the kinetic resistance would produce an additional term in initial diameter. The char burnout times, which were measured visually, were plotted against the square of the initial particle diameter, cf. equation (E.2.4). Based on the straight line plots obtained they concluded that the combustion process was indeed controlled by the film diffusion resistance.

It has been pointed out by Tomeczek (1979) that the burnout time data of Avedesian et al would also produce acceptable straight line plots if plotted against the initial particle diameter. Straight line plots of this nature would indicate that the kinetic resistance was limiting.

The research work of Ross & Davidson (1981) considered the combustion of char particles in the temperature range of 1183 to 1173 K in order to establish the relative importance of film diffusion and reaction kinetics in determining the rate of combustion. They derived three combustion models, which were all based on the two phase theory of fluidization. Furthermore, all the models incorporated both the film diffusion and kinetic resistances. The models differed in their approach to the combustion reaction mechanism. The mechanisms considered were the two film reaction mechanism, the direct oxidation reaction mechanism assuming the CO reaction to proceed rapidly and the direct oxidation mechanism assuming the CO reaction to proceed slowly. The derived burnout time expressions were similar to equation (E.2.4), except for an additional kinetic resistance term which contained the surface reaction rate constant. Their theoretical analysis resulted in the following relation between the overall combustion resistance ($1/K$) and the parameters of the kinetic resistance (K_C) and the film diffusion resistance (Sh).

$$\frac{1}{K} = \frac{\gamma}{K_C} + \frac{\alpha D}{Sh D_0} \quad \text{----- (E.2.5)}$$

γ and α are constants whose values depend on which reaction mechanism is assumed to occur. The experimental

results of Ross & Davidson (1981) clearly showed that both the reaction kinetics and the diffusion of oxygen through the gas film are important in determining the rate of combustion. The values of the Kinetic (K_c) and film diffusion (Sh) parameters were evaluated using the experimental combustion rates and equation (E.2.5). The values obtained for the reaction rate constant indicated that the occurrence of the Boudourd reaction at the surface, cf. two film mechanism, was not possible at the bed temperatures employed. The rate constant values were consistent with the surface reaction of the direct oxidation reaction mechanism, viz. $C + \frac{1}{2}O_2 \rightarrow CO$. The results of Ross & Davidson (1981) suggested different reaction mechanisms for large and small particles. For large particles the CO was oxidised close to the surface which resulted in particle temperatures in excess of the bed temperature. For small particles the CO burnt in the particle surroundings and the "reaction energy" was dissipated by the inert bed material. Consequently the smaller particles exhibited a temperature close to that of the bed. Ross & Davidson concluded that the combustion of large particles is primarily controlled by the film diffusion resistance while the combustion of small particles is largely controlled by the kinetics of the surface reaction. The nature of the limiting resistance been attributable to the surface temperature of the particles.

Pillai (1981) experimentally determined the devolatilization and char burnout times for the batch wise fluidised bed combustion of twelve different coal types. Pillai (1981) considered the total burnout time of the coal particles (τ_b) to consist of a volatiles combustion component and a char combustion component, viz :

$$\tau_b = \tau_v + \tau_c \text{ ----- (E.2.6)}$$

The char combustion time was visualised to consist of a further two components, namely an interphase oxygen transfer time (τ_i) and a particle size dependent time (τ_s), viz :

$$\tau_c = \tau_i + \tau_s \text{ ----- (E.2.7)}$$

where $\tau_i = \frac{\xi M_c}{C_o}$ and $\tau_s \approx p D^m$

Equation (E.2.7), which is similar in form to equation (E.2.4), considers the hydrodynamic characteristics and the combustion resistances as lumped parameters, i.e. ξ and p , respectively. For $m=1$ the surface reaction kinetics are limiting, while for $m=2$ the film diffusion resistance is limiting. Although the theoretical approach is rather empirical, the subsequent analysis of the experimental results was capable of broadly quantifying the relative roles of the combustion resistances for the coal types examined. The conclusions reached by Pillai (1961) are summarised above in section 2.2.1.

3. THEORY

The combustion process of coal particles in a fluidized bed may be visualized as comprising of two distinct phases, namely, a devolatilization phase and a char combustion phase. Thus the total combustion time of a given coal sample may be written as :

$$\tau_b = \tau_v + \tau_c \quad \text{----- (E.3.1)}$$

The devolatilization time (τ_v) represents the total time required for the release and combustion of the volatile matter of the coal. A mathematical consideration of the time dependant characteristics of a devolatilizing coal particle can prove to be extremely complex. The volatiles combustion process is modelled by using the simple correlation of Pillai (1981), which relates the devolatilization time to the initial diameter of the coal particle.

The expressions relating the char combustion time (τ_c) to the experimental conditions are based on a collective consideration of the fluidized bed hydrodynamics, the char combustion resistances and the char reaction mechanisms. The combustion of coal typically follows a shrinking particle mode of reaction, however for high ash content coals a shrinking core mode of reaction is necessary. Both modes of reaction are considered in the theoretical analysis. The reactor hydrodynamics are described using the two-phase theory of Davidson & Harrison (1963). The hydrodynamic expressions are used to describe the transfer of oxygen from the bubble phase to the particulate phase, which constitutes the convective mass transfer resistance. The theoretical analysis considers the overall combustion process to be controlled by various resistances in series such as the film diffusion of oxygen, the rate of the surface reaction and, where applicable, the diffusional resistance of the ash layer. The combustion of carbon to carbon dioxide is described by the direct oxidation mechanism as employed by Ross & Davidson (1981).

3.1 THE TWO PHASE THEORY OF FLUIDISATION.

The two phase theory of fluidisation, originally introduced by Davidson & Harrison (1963), considers a fluidized bed as a two phase system. The two phase system consists of a particulate phase and a bubble phase. The flowrate of gas through the particulate (or emulsion) phase is equated to the incipient fluidization flowrate. The bubble phase carries the additional fluidising gas. The hydrodynamic model used in this investigation is based on the two phase fluidisation theory and assumes the particulate phase to be perfectly mixed and the bubble phase to be in plug flow.

The flue gas component concentrations are obtained by considering a material balance over the two phase system. The derivation of the relevant equations are given by Davidson & Harrison (1963) and the fluidized bed system is shown in figure 3.1.

The reactant concentration in the bubble phase is obtained by considering a mass balance on a single rising bubble. The following relation between the reactant concentration and the height above the distributor is obtained:

$$C_b = C_p + (C_0 - C_p) \exp(-Q y / U_b V) \quad \text{----- (E.3.2)}$$

where : $Q = q + k_g S$

C_b - reactant concentration in the bubble phase at a height y above the distributor.

C_0 - reactant inlet concentration.

C_p - reactant concentration in the particulate phase.

k_g - the mass transfer coefficient between the main bubble volume and the bubble wall.

q - the volume flowrate in and out of the bubble.

S - the bubble surface area.

U_b - the bubble velocity

V - the bubble volume.

y - the height above the distributor

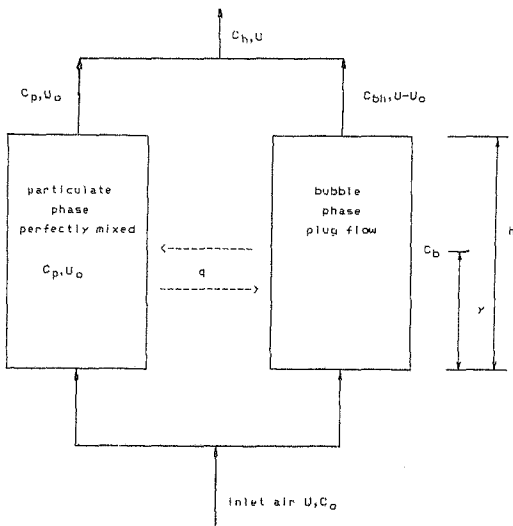


Figure 3.1 Fluidized bed reactor according to the two phase theory

A material balance over the particulate phase (considering the reactant to be consumed by a first-order reaction) results in the following expression :

$$(C_0 - C_p) (U - (U - U_0) \exp(-X)) = k H_0 C_p \quad \text{----- (E.3.3)}$$

where k is defined in the following equation as

$$\begin{aligned} \text{total rate of oxygen consumption} &= k C_p \\ \text{per unit volume of particulate phase} & \end{aligned}$$

and the cross flow factor X is defined as :

$$X = Q H_0 / U_0 U$$

An overall mass balance over the reactor is given by equation (E.3.4), viz :

$$U C_h = (U - U_0) C_{bh} + U_0 C_p \quad \text{----- (E.3.4)}$$

The fraction of reactant in the flue gas is found by combining equations (E.3.2), (E.3.3) and (E.3.4) to give the following equation :

$$C' = \frac{C_h}{C_0} = \beta \exp(-X) + \frac{(1 - \beta \exp(-X))^2}{k' + 1 - \beta \exp(-X)} \quad \text{----- (E.3.5)}$$

$$\begin{aligned} \text{where } \beta &= 1 - U_0/U \\ k' &= k H_0/U \end{aligned}$$

The parameter X represents the number of times the bubble volume is swept out during its time in the reactor. The importance of the convective mass transfer resistance is governed by the magnitude of the parameter X . If $X \rightarrow \infty$, which implies very good mixing between the two phases, equation (E.3.5) reduces to the standard mixed flow reactor (DSTR) expression, viz $C' = 1/(k' + 1)$. If the rate of the reaction is very large, i.e. $k' \rightarrow \infty$, then the fractional

conversion is limited by the value of $\beta \exp(-X)$. Complete conversion of the reactant is only possible if perfect mixing is attained, which eliminates by passing of the reactant.

The rate of reactant oxygen consumption is given by equation (E.3.6).

$$\text{rate of reactant consumption} = A_r (C_0 - C_p) \langle U - (U - U_0) \exp(-X) \rangle \quad \text{----- (E.3.6)}$$

The equations mentioned above incorporate the hydrodynamic characteristics of a fluidised bed in the form of mass balance expressions which enable one to calculate the reactant exit concentrations for specified operating conditions. To perform such calculations one requires further information with regards to the dimensionless reaction rate constant (k'). The development of reaction rate expressions relevant to the fluidised bed combustion of coal particles are discussed in sections 3.2 and 3.3 below.

3.2 COAL DEVOLATILIZATION.

As previously mentioned the release and combustion of coal volatiles is extremely complex. It was considered appropriate, in terms of the objectives of this project, to consider only the total time required for the devolatilization to occur.

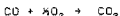
The devolatilization time may be expressed as follows (this formula was verified experimentally by Pillai (1981)) :

$$\tau_v = a D_1^v \quad \text{----- (E.3.7)}$$

The parameters a and v are dependent upon the nature of the coal. The values of a and v used to describe the devolatilization process of the Tavistock duff and Rietspruit discard coals are given in section 6.2.

3.3 Combustion of char.

The theoretical aspects of coal combustion presented below are concerned with the derivation of expressions which relate the particle diameter and the flue gas oxygen concentration to the combustion time. Two modes of reaction are considered. Typically the coal combustion follows either a shrinking particle mode of reaction or a shrinking core mode of reaction for high ash content coals. The char combustion mechanism is assumed to follow the direct oxidation sequence i.e.



The derivation of the combustion models is based on the following strategy :

- an expression for the flux of oxygen to the carbon surface is derived, considering the geometry of the char particle and concentration profiles in its surroundings.
- the rate of carbon consumption at the char surface is then equated to the flux of oxygen. A factor b is incorporated to represent the reaction mechanism. The resulting expression relates the overall combustion resistance to the individual resistances which act in series.
- the overall combustion resistance equation is then related to the dimensionless reaction constant (k') as specified in equation (E.3.4)
- the diameter-time relationship is found by the simultaneous solution of the equation for the total rate of oxygen consumption and the equation for the total rate of carbon consumption. The particulate phase oxygen concentration is eliminated to yield an expression of the char particle diameter as a function of time.

3.3.1 Shrinking particle combustion model.

The derived shrinking particle combustion model considers both the film diffusional and reaction kinetic resistances to be important.

Consider a single spherical char particle which reacts according to the direct oxidation mechanism. The oxygen concentrations in the particulate phase and at the surface of the char particle are denoted by C_p and C_s , respectively. The flux of oxygen through the gas film layer to the char surface is thus given by :

$$n = \pi D^2 k_g (C_p - C_s) \quad \text{----- (E.3.8)}$$

A Sherwood number may be defined in terms of the mass transfer coefficient (k_g) as :

$$Sh = \frac{k_g D}{D_g} \quad \text{----- (E.3.9)}$$

Combining equations (E.3.8) and (E.3.9) one obtains the following :

$$n = \pi Sh D_g D (C_p - C_s) \quad \text{----- (E.3.10)}$$

An overall rate constant (K) may be defined in terms of the carbon combustion rate (R_c) :

$$R_c = \pi D^2 K C_p \quad \text{----- (E.3.11)}$$

where

$$R_c = - \frac{\pi \rho_c D^2}{24} \frac{d(D)}{dt}$$

Similarly, the surface reaction rate constant may be defined as :

$$R_c = \pi D^2 k_c C_s \quad \text{----- (E.3.12)}$$

The direct oxidation mechanism consists of two distinct reaction sequences, depending on the location of the CO combustion reaction. The sequence representing the complete combustion of CO at the particle surface is denoted as mechanism 1. The reaction sequence representing the combustion of CO in the particle surroundings is denoted as mechanism 2. The relationship between the total rate of carbon consumption at the surface of the particle and the flux of oxygen to the surface is fixed by the stoichiometry of the effective surface reaction. A general equation may be expressed as follows :

$$R_c = b n \quad \text{----- (E.3.13)}$$

where : $b = 1$ for mechanism 1
 $b = 2$ for mechanism 2

Substituting the equations (E.3.10), (E.3.11) and (E.3.12) into equation (E.3.13) the following expression for the overall rate constant (K) is obtained :

$$\frac{1}{K} = \frac{1}{k_c} + \frac{D}{b \text{ Sh } D_g} \quad \text{----- (E.3.14)}$$

The parameter $1/K$ is commonly referred to as the overall combustion resistance. The dimensionless rate constant (k') of equation (E.3.5) may be expressed in terms of the overall rate constant of the single particle (K) by considering the total rate of oxygen consumption for a batch of N char particles. For the complete oxidation of carbon to carbon dioxide one may write :

$$\text{total rate of oxygen consumption} = \text{Total rate of carbon consumption}$$

ie.

$$A_r U k' C_p = N R_c \quad \text{----- (E.3.15)}$$

Expressing the number of particles in terms of the mass of carbon charge (M_c) and substituting (E.3.11) into (E.3.15) one obtains the following expression for K' :

$$K' = \frac{\delta M_c K D^2}{\rho_c A_r U D_j^3} \quad \text{----- (E.3.16)}$$

Equation (E.3.6), which relates the total rate of oxygen consumption in terms of the reactor hydrodynamics, may be equated to the LHS of equation (E.3.15) to obtain an expression for the particulate phase concentration in terms of K' , viz.

$$C_p = \frac{C_o A}{A + A_r U K'} \quad \text{----- (E.3.17)}$$

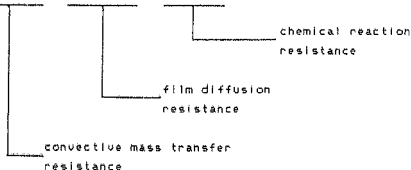
where : $A = A_r (U - (U - U_o) \exp(-X))$

Substituting equation (E.3.17) into equation (E.3.11) one obtains an expression for the diameter of the char particle as a function of time only, ie :

$$- \frac{d(D)}{dt} = \frac{24 C_o A K}{\rho_c (A + A_r U K')} \quad \text{----- (E.3.18)}$$

The Sherwood number in equation (E.3.18) may be considered either as a constant or as a function of the particle diameter. Upon substitution of the expressions for K and K' , equation (E.3.18) may be integrated to yield the following diameter time relationship (assuming the Sherwood number to be a constant w.r.t. the particle diameter) :

$$t_c = \frac{C_0 \times (1-x^3)}{3} + \frac{C_1 \times (1-x^2)}{2} + \frac{C_2 \times (1-x)}{1} \quad \text{----- (E.3.19)}$$



where:
$$C_0 = \frac{M_c}{12 C_o A_p (U - (U - U_o) \exp(-X))} \quad \text{----- (E.3.20)}$$

$$C_1 = \frac{\rho_c D_i^2}{48 b C_o Sh D_p} \quad ; \quad b=1 \text{ or } 2 \quad \text{----- (E.3.21)}$$

$$C_2 = \frac{\rho_c D_i}{24 C_o k_c} \quad \text{----- (E.3.22)}$$

$$x = \frac{D}{D_i} \quad \text{----- (E.3.23)}$$

The value of b in equation (E.3.21) indicates the value of the molar flowrate of oxygen to the char particle surface. For b=1 the overall combustion of carbon to carbon dioxide at the char surface is complete, whereas for b=2 the production of carbon dioxide occurs at some distance from the char surface.

When x=0, equation (E.3.19) gives the char burnout time T_c as specified below.

$$T_c = C_0 + C_1 + C_2 \quad \text{----- (E.3.24)}$$

If the rate of the surface reaction is very fast then term C_2 tends to zero and if b=2, then equation (E.3.19) reduces to the film diffusion combustion model of Avedesian & Davidson (1973).

Further it is possible to modify the film diffusion resistance term in equation (E.3.19) to account for the variation of the Sherwood number with particle size. The dependance of the Sherwood number on the particle diameter is given by equation (E.3.25), which is the Sherwood correlation of Ranz & Marshall (1952).

$$Sh = 2 + 0.6 Sc^{1/3} Re^k \quad \text{----- (E.3.25)}$$

The above Sherwood correlation may be used to replace the Sherwood number in equation (E.3.14). The integration of equation (E.3.18), assuming a variable Sherwood number, results in the following time-diameter relationship :

$$t_c = C8*(1-x^3) + C2*(1-x) + z*y*(1-x^2) - \frac{y^2*(1-x)}{2} + \frac{y^3*(1-x^3/2)}{3} - \ln\left(\frac{1+y}{1+y^2}\right) \quad \text{----- (E.3.26)}$$

where :

$$z = \frac{P_c}{24 C_0 D_0 y^2} \quad \text{----- (E.3.27)}$$

$$y = 0.3 Sc^{1/3} Re^2 \quad \text{----- (E.3.28)}$$

The convective mass transfer term (C8) and the chemical reaction resistance term (C2) in equation (E.3.26) are identical to those presented in equation (E.3.19). The film diffusion resistance term is somewhat more complex as a result of introducing the Sherwood correlation, which incorporates the particle diameter in a Reynolds number term.

The shrinking particle combustion model may be represented in various forms, depending on the selected assumptions. The above theoretical analysis identifies three basic forms of the combustion model. These are as follows:

- film diffusion and kinetic resistances with a constant Sh number.
- film diffusion and kinetic resistances with a variable Sh number.
- film diffusion resistance only, i.e. the Avedesian and Davidson model.

3.3.2 shrinking core combustion model.

The shrinking core combustion model presented below, is obtained by selecting the diffusion of oxygen through the ash layer and the kinetics of the surface reaction as the predominant combustion resistances. Furthermore the direct oxidation reaction approach is also assumed to be applicable.

The flux of oxygen diffusing through the ash layer to the char surface is given by Levenspiel (1972) as :

$$n = - 2\pi D^2 D_e \frac{dC}{dD} \quad \text{----- (E.3.29)}$$

Equation (E.3.29) may be integrated, using the following boundary conditions. :

$$\begin{array}{ll} \text{at } D = D_i & C = C_p \\ & D = 0 & C = C_s \end{array}$$

to yield the following expression for n :

$$n = 2\pi D_e (C_p - C_s) \frac{D_i D}{(D_i - D)} \quad \text{----- (E.3.30)}$$

The overall rate constant (K) is defined in terms of the rate of carbon consumption (based on the external surface area of the char particle), viz.

$$R_c = \pi D_i^2 K C_p \quad \text{----- (E.3.31)}$$

The definition of the surface reaction rate constant is the same as for the shrinking particle model i.e.(E.3.12). An expression for the overall combustion resistance ($1/K$) is obtained by substituting equations (E.3.12), (E.3.20) and (E.3.31) into equation (E.3.13), viz:

$$\frac{1}{K} = \frac{D_1^2}{K_c D^2} + \frac{D_1 (D_1 - D)}{2 b D_e D} \quad \text{----- (E.3.32)}$$

An expression for the dimensionless rate constant (K') is obtained in a similar fashion to equation (E.3.16), viz:

$$K' = \frac{6 M_c K}{P_c A_r U D_1} \quad \text{----- (E.3.33)}$$

The diameter time relationship is found by substituting equation (E.3.17) into equation (E.3.31) to produce the following

$$-\frac{d(D)}{dt} = \frac{24 D_1^2 C_0 A K}{P_c D^2 (A + A_r U k')} \quad \text{----- (E.3.34)}$$

Equation (E.3.34) may be readily integrated to yield the following diameter-time expression :

$$t_c = C_0 \times (1-x^3) + C_3 \times (1-3x^2+2x^3) + C_2 \times (1-x) \quad \text{----- (E.3.35)}$$

where :

$$C_3 = \frac{P_c D_1^2}{288 v_g C_0} \quad \text{----- (E.3.36)}$$

The burnout time expression is the same as equation (E.3.24). The definitions of C_0 and C_2 are identical to those listed in equations (E.3.20) and (E.3.22), respectively.

4. ASSUMPTIONS AND CALCULATION PROCEDURE.

The combustion theory presented in section 3 relates the coal sample characteristics (eg. particle diameter and mass of fixed carbon) and the reactor operating conditions (eg. gas velocity and bed temperature) to the burnout time and the flue gas components concentration. The main objective of this investigation is to measure experimentally, the burnout times and flue gas concentrations, for various values of the combustion variables, which are quoted in parenthesis above. Following this an attempt is to be made to describe the combustion process both in qualitative and mathematical terms. The end result of this investigation is to provide one with a method of predicting the events of a combustion process, given a set of coal characteristics and operating conditions.

The mathematical description of the combustion process involves the evaluation of the unknown model parameters by regression of the plots of the burnout time versus mass of carbon charge. These evaluated parameters may then be substituted into the appropriate model equations to yield the prediction of the flue gas carbon dioxide concentration as a function of time. Comparison of the theoretical and experimental carbon dioxide traces will enable one to establish which combustion model represents best the combustion process under the conditions investigated. The assumptions and procedures required to perform these calculations are outlined below.

4.1 CALCULATION ASSUMPTIONS.

- (1) The elutriated bed material captured by the cyclone during a single experiment has a typical mass of between 2 and 5 grams and a carbon content in the range of 1.0-4.0 %. In calculating the mass of carbon charged the mass of elutriated carbon is assumed to be negligible. (See appendix D.)

- (ii) The coal charged into the fluidized bed is assumed to devolatilize completely and the remaining char consists of only fixed carbon and inert ash. The proportions of carbon and ash in the residual char is assumed to be given by the proximate analysis of the coal. Furthermore the charged coal is assumed to neither swell nor fracture during the combustion process. Attrition of the coal particles is assumed to be negligible.
- (iii) The devolatilization process of coal particles is assumed to occur either instantaneously i.e. $\tau_d=0$ or in a small finite time as given by the expression of Pillai (1981) i.e. $\tau_d = a D_p^v$. Furthermore it is assumed that during the devolatilization of the coal the extent of the fixed carbon combustion is negligible and that the particle diameter remains constant.
- (iv) The burnout time of the coal sample is assumed to be given by the time from the beginning to the end of the carbon dioxide trace. The burnout time of the char is then given by the difference between the coal burnout time and the assumed devolatilization time.
- (v) During char combustion the flue gas is assumed to contain only nitrogen, oxygen and carbon dioxide. The inlet air is assumed to be dry and have an oxygen concentration of 21.8% (mol basis).
- (vi) The gas phase diffusion coefficient is calculated using the Chapman-Enskog equations as Leonard-Jones parameters as referenced by Strehlow (1968). The inlet oxygen concentration is calculated using the ideal gas law. The value of the pressure just above the gas distributor is used in the above calculations and was found to have a value of approximately 85kPa (abs).

(vii) The minimum fluidization velocity was experimentally determined using two methods. The first method being a series of bed pressure drop determinations at various gas flowrates. The second method used was to measure the temperature at which the lower part of bed became fluidized. This temperature was indicated by a thermocouple placed near the gas distributor. When this region becomes fluidized the temperature of this lower region increases dramatically. Thus since the air mass flowrate was known the gas velocity at this temperature could be calculated.

(viii) The coal combustion process is assumed to occur under isothermal conditions. The bed temperature rise, which naturally accompanies coal combustion, was found to be relatively small. (See appendix E.)

The physical constants used in the evaluation of the combustion equations are listed in table 4.1 for the various operating conditions encountered.

Table 4.1 Values of physical constants used in the experimental data regression.

Bed temperature degrees Celsius T_b	Rotameter height cm R_t	Gas velocity (bed) m/s U	Inlet O_2 conc. $\times 10^{-2}$ kmol/m ³ C_0	Diffusion coefficient m ² /s $\times 10^{-3}$ D_0
526	12	.2624	0.2734	0.1264
715	4	.1473	0.2195	0.1821
	6	.1981		
	8	.2329		
848	6	.2141	0.1948	0.2219

Incipient fluidizing velocity : $U_0 = 0.0964 \text{ m/s}$
 Fluidized bed cross-sectional area : $A_p = 43.86 \times 10^{-4} \text{ m}^2$

4.2 REGRESSION ALGORITHM TO DETERMINE THE MODEL PARAMETERS.

The regression algorithm proposed is rather standard and involves the determination of the parameters Sh and k_c from a plot of the burnout time versus the mass of carbon charge and using equation (E.3.24). The coefficient C_0 in equation (E.3.24) contains the mass of carbon charge (M_C) and the cross flow factor X . The coefficients C_1 and C_2 respectively contain the Sherwood number (Sh) and the surface reaction rate constant (k_c). Typically the slope of these plots is used to determine the value of X , while the "y-intercepts" are used to determine the values of Sh and k_c .

During the regression of the experimental data one is not concerned with the problem of which reaction mechanism prevails, since the regression analysis only evaluates the model coefficients, namely C_0 , C_1 and C_2 . For the sake of consistency and comparison with the Avedesian and Davidson model, the parameter b is equated to 2 in order to facilitate the calculation of the Sherwood number during the regression analysis. It is intended to investigate the question of which reaction mechanism prevails only once the particular form of the general combustion model has been established. The approach used here was to incorporate all the data points in order to evaluate Sh and k_c . The sum of the squared errors is defined by equation (E.4.1).

$$S = \sum_j (\tau_j - C_0 j - \frac{\omega_j}{Sh} - \frac{\nu_j}{k_c})^2 \quad \text{----- (E.4.1)}$$

where :

$$C_0 j = \frac{F_c M_{Cj}}{12 C_0 A_r (U_j - (U_j - U_0) \exp(-X))}$$

$$\omega_j = \frac{\rho_c (D_{1j})^2}{96 D_g C_0}$$

$$\nu_j = \frac{\rho_c D_{1j}}{24 C_0}$$

The S_h and K_c values for a minimum sum of squared errors are given by equations (E.4.2) and (E.4.3), respectively.

$$S_h = \frac{\sum y^2 \sum w^2 - (\sum wy)^2}{\sum w^2 \sum v^2 - \sum vw \sum vf} \quad \text{----- (E.4.2)}$$

$$K_c = \frac{\sum y^2 \sum w^2 - (\sum wy)^2}{\sum vf \sum v^2 - \sum vw \sum wf} \quad \text{----- (E.4.3)}$$

where $f = T_j - C_{O_j}$

The value of X was iteratively chosen to obtain a minimum S value. It is possible to derive a set of equations similar to (E.4.2) and (E.4.3) which would simultaneously solve for X , S_h and K_c such that S is a minimum. However, for programming simplicity as well as flexibility, the iterative method was chosen.

A program to perform this regression algorithm is listed in appendix B (program MOD).

4.3 PREDICTION OF CARBON DIOXIDE IN THE FLUE GAS.

The theoretical prediction of the oxygen or carbon dioxide trace involves the following procedure:

- specify a particle diameter D between D_1 and zero.
- evaluate the time t_c from say equation (E.3.19)
- add the devolatilization time T_v (E.3.7) to obtain T_0 from (E.3.1).
- evaluate the dimensionless rate constant K' for the specified diameter D from (E.3.16).
- evaluate C_h from equation (E.3.5) by substitution of K' and the experimentally determined cross-flow factor X .

The carbon dioxide concentration, during char combustion, is simply 0.21 minus the oxygen concentration. A program employing the above procedure is listed in appendix B, (program TRACE).

5. EXPERIMENTAL PROCEDURE.

In this experimental investigation the combustion of two types of coal, namely Tavistock Duff and Rietspruit Discard, have been considered in the temperature range 520 °C - 840 °C. The majority of the data consists of the combustion of Tavistock Duff at 715 °C. Although this temperature represents the lower operating conditions of large scale fluidized beds, it was found to be a practicable temperature to use in running the experimental fluidized bed. Greater priority was given to the combustion of Tavistock coal because it is the intention to use it as the primary coal feedstock in the NFBC demonstration boiler project.

The experimental work was carried out on a laboratory scale fluidized bed, which has an internal diameter of 76mm. A sketch of the fluidized bed system is given in figure 5.1. Dimensioned drawings of the fluidized bed reactor are given in appendix F. The reactor was externally heated by electrical elements. The bed temperature was controlled using a variac and a Eurotherm temperature controller. The fluidizing air was supplied from a compressed air line and the flowrate was measured using a GEC 14E rotameter. Numerous temperatures (see figure 5.1) were continuously monitored on a chart recorder. The flue gas analysis equipment comprised a paramagnetic oxygen analyser and an infrared carbon dioxide analyser. Prior to a batch of experiments the reactor was filled with inert bed material, namely -1 mm sand, to a height of 280 mm. A typical experiment consisted of the following events :

- a) preheating the reactor to the required bed temperature and selection of the required fluidizing velocity.
- b) inserting a coal sample of known mass and particle size into the bed via a double valve system.
- c) monitoring on a continuous basis the flue gas oxygen and carbon dioxide concentrations, and
- d) recovering from the cyclone dropout cylinder all the elutriated bed material for carbon content analysis.

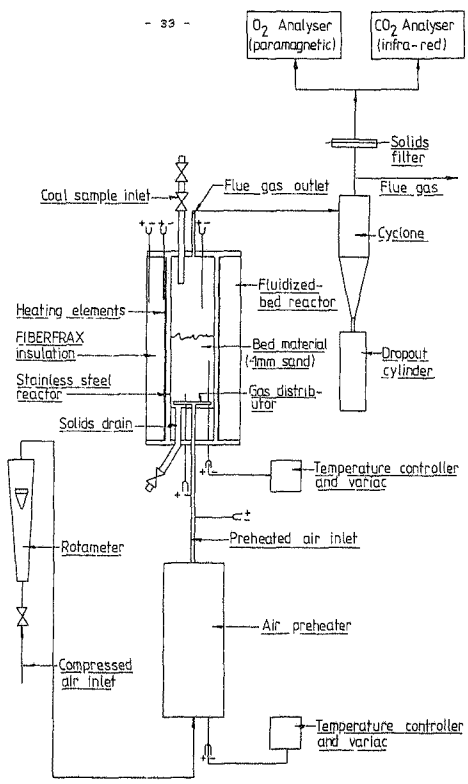


FIGURE 5.1: FLUIDIZED-BED REACTOR SYSTEM.

The burnout time of the coal sample was read off the chart of the carbon dioxide trace. (This method of determination has been compared with other methods, such as the visual observation of the burning particles, by Chakraborty & Howard (1981) and was found to be satisfactory.)

The operating conditions of the experimental fluidized bed are summarised in table 5.1, while the coal sample characteristics are listed in table 5.2. The standard sieve sizes for sizing the coal samples are given in table 5.3.

Table 5.1 Operating conditions.

Bed temperature celsius T_b	Air inlet flowrate g/s	Gas velocity m/s U	Rotameter height R_t cm
520	0.434	0.2626	12
	0.196	0.1473	4
715	0.252	0.1901	6
	0.389	0.2329	8
910	0.252	0.2141	6

Table 5.2 Coal characteristics.

Proximate analysis	Tavistock Duff	Rietspruit Discard
% moisture	3.3	2.3
% volatile matter	25.8	16.5
% fixed carbon	54.4	21.2
% ash	16.5	60.0
coal density Kg/m ³	1365.8	2012.0
cal. val MJ/Kg	25.8	9.5

Table 5.3 Coal particle diameters.

Upper and lower sieve sizes	Mean diameter D_j /mm
-1.18 +1.0	1.09
-2.36 +2.0	2.18
-2.8 +2.36	2.58
-3.35 +2.8	3.08
-5.0 +4.0	4.5

6. ANALYSIS OF THE EXPERIMENTAL COMBUSTION RESULTS.

The burnout times and masses of the coal samples are listed in appendix A. The data analysis has been broadly divided into two sections namely a qualitative description and a mathematical description of the data.

The qualitative description considers the trends exhibited by the data and discusses whether these trends are consistent with those expressed in the literature. Comparisons of the combustion behaviour under various operating conditions are made and the influence of these various conditions are explained.

The mathematical description involves the application of suitable regression methods to the experimental data in order to establish the values of the various unknown parameters of the proposed combustion models. The theoretical models and the combustion behaviour are compared and a decision is made as to which model best represents the combustion behaviour of the coal types investigated.

Discussions relevant to the two sections mentioned above are expanded below to create a deeper understanding of the combustion behaviour of Rietspruit Discard and Tavistock Duff coals in a fluidized bed.

6.1 QUALITATIVE DESCRIPTION.

The combustion of coal is strongly influenced by the fluidized bed operating conditions and the characteristics of the coal sample. The effect of these various parameters are discussed in depth below.

6.1.1 THE EFFECT OF THE FLUIDIZED BED OPERATING CONDITIONS ON COMBUSTION.

The fluidized bed reactor conditions may be characterised by the bed temperature, the gas velocity, the bed height and diameter and the inert particle size. These factors play an important role in determining the hydrodynamic behaviour of the fluidized bed, which in turn influences the combustion behaviour of a particular coal sample. The effects of these various factors on the combustion process are discussed below.

The temperature dependence of the combustion process is shown in figure 6.1. As it is expected an increase in temperature results in an increase in the combustion rate and accordingly a decrease in the burnout time. At 528 °C burnout times become markedly larger than those at 840 °C. This trend indicates that the overall combustion rate at relatively low temperatures becomes strongly dependant on the rate of the reaction itself. Furthermore this trend is less pronounced for the high ash content discard coal which indicates that although the rate of the chemical reaction decreases, with decrease in temperature, a further resistance, which is less dependant on temperature, is responsible for the control of the overall combustion rate. This is probably caused by the diffusion resistance of oxygen through the ash layer. Superimposing the oxygen traces for two samples burnt at different temperatures (see figure 6.2) one may note that higher temperatures result in a much faster rate of devolatilization and char combustion.

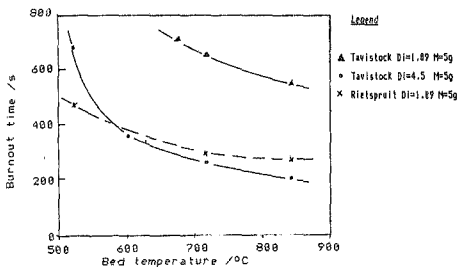


Figure 6.1 Burnout time versus bed temperature.

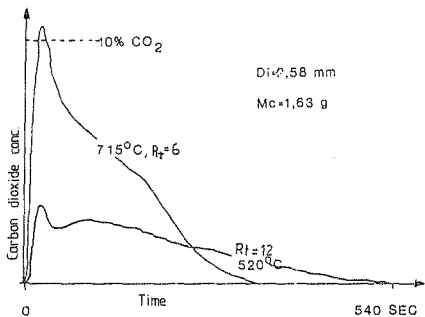


Figure 6.2 Effect of temperature on the combustion of Tavistock Duff.

Furthermore the traces at 520 °C display a regular pattern of a second peak emerging after the initial devolatilization peak. The existence of the second peak tends to indicate that the time required for the establishment of char combustion exceeds that required for devolatilization. As the temperature increases, a single peak emerges which probably comprises of both volatiles and char combustion.

An increase in the fluidizing velocity results in a decrease in the burnout time as shown in figure 6.3. This trend is expected since a greater air flowrate not only provides a larger excess of oxygen, it also increases the rate of oxygen transfer from the bubble phase to the particulate phase where most of the char combustion occurs. At large velocities and hence large mass transfer rates one would expect the burnout time to tend to a constant value. While at incipient fluidization (dashed line in figure 6.3) one would expect the burnout time to dramatically increase as a result of the "poor mixing" and low mass transfer rates between the bubble and particulate phases. In addition, at such low velocities the attrition of the ash layer surrounding the burning particle is likely to be small, hence the combustion rate would be retarded. Extrapolation of the curves in figure 6.3 confirms the postulations outlined above.

An increase in the static bed height would proportionally increase the value of the parameter X, as implied by equation 6.21 of Davidson & Harrison (1963). An increased X value would decrease the "hydrodynamic resistance" and the burnout time. (Care was taken throughout the experimental program to keep the static bed height and the inert particles size distribution constant.)

6.1.2 THE EFFECT OF THE COAL CHARACTERISTICS ON COMBUSTION

The following characteristics are thought to be of importance in describing the combustion behaviour of a coal sample. These are the particle diameter, the coal sample mass, the coal type and the volatile matter content. The effects of these various parameters on the combustion process is discussed below.

Plots of the burnout time versus particle diameter and the square of the diameter are presented in figures 6.4 and 6.5, respectively. The carbon dioxide traces for samples having various diameters are superimposed in figure 6.6. Since the particle surface reaction area per unit mass decreases with an increase in the particle diameter, the burnout time increases with increasing particle diameter. This behaviour as implied in all the theoretical models is depicted quite clearly in figures 6.4 and 6.6. The nature of these curves aids in establishing the relative roles of the various rate controlling mechanisms on the overall combustion rate. One may write the following expression to generally describe the curves :

$$\tau_c \propto D_p^m$$

If m is equal to one the rate controlling mechanism is the chemical reaction, while if m is equal to two the film diffusion of oxygen is limiting closely (considering a shrinking particle mode of reaction). It is interesting to note that if one assumes a shrinking core mode of reaction, and if $m=2$, then one would deduce that diffusion of oxygen through the ash layer is limiting. Values of m between one and two indicate a combination of effects which control the overall reaction. Avedesian and Davidson, (1973) obtained acceptable straight line plots of τ_c versus D_p^2 and deduced that the combustion process is purely film diffusion controlled. However, Tomczek (1979) has shown that they could have also obtained acceptable straight line plots of τ_c versus D_p . Comparing figures 6.4 and 6.5, one notes that the plot

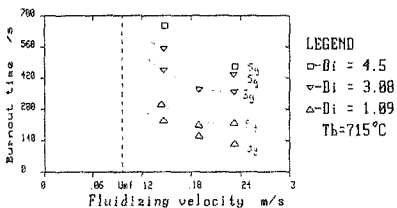


Figure 6.3 Tavistock burnout line versus fluidizing gas velocity.

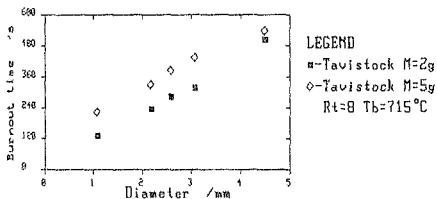


Figure 6.4 Burnout time versus diameter.

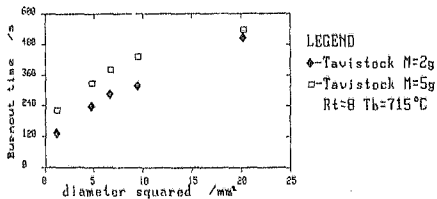


Figure 6.5 Burnout versus diameter squared.

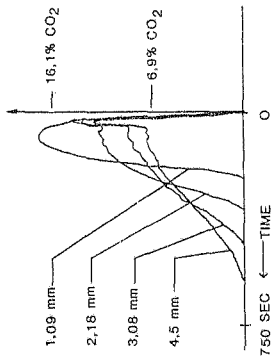


Figure 6.6

EFFECT OF PARTICLE DIAMETER ON
THE COMBUSTION OF TAVISTOCK
DUFF.

$T_b = 715^\circ\text{C}$

$U = 0.233 \text{ m/s}$

$M_c = 3.54 \text{ g}$

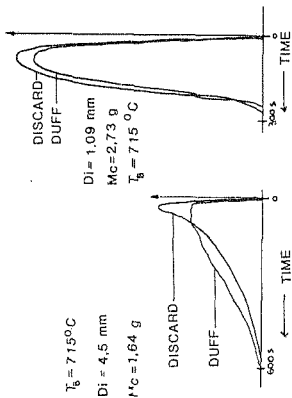


Figure 6.7

COMPARISON OF CO₂ TRACES OF
RIETSPRUIT DISCARD AND TAVISTOCK
DUFF.

against particle diameter has a higher degree of linearity than the plot against the particle diameter squared. On the basis of the work by Tomeczek (1979) one will be incorrect to presume then that the combustion process is controlled by the kinetic resistance. It is believed that a data analysis based purely on the particle diameter-burnout time characteristics is insufficient to clarify the mechanism of the combustion reaction. However, it is probably safe to say that the combustion process of the Tavistock coal is not purely film diffusion controlled.

At 715 °C, experiments were carried out using six different masses and five different diameters. The results are shown in the relevant figures in section 6.2. In stating the obvious one observes that an increase in the carbon mass results in an increase in the burnout time. The plots of T_c versus M_c produce reasonable straight lines, as is also indicated by the combustion models. Furthermore the lines are reasonably parallel which tends to indicate that the cross flow factor (parameter X) remains more or less constant over the range of operating conditions employed. The y-axis intercepts, represent the characteristics of single particle combustion process i.e. conditions where M_c is very small.

There is a distinct difference between the combustion behaviour of the Tavistock and Rietspruit coals (see figure 6.7), particularly for the larger diameter particles. The shapes of the carbon dioxide traces for Rietspruit discard and Tavistock Duff are generally concave and convex, respectively. A concave shaped trace indicates that a particular combustion resistance is increasing as the extent of the reaction increases. Diffusional resistance of oxygen through an ash layer would create such an effect. As the initial particle size decreases the ash layer resistance plays a diminishing role. For the 1.09 mm particle size range the combustion characteristics of Tavistock and Rietspruit coals are similar (see figure 6.7) which indicates that both coals experience similar combustion resistances. Film diffusion and ash layer diffusion

resistances possibly play diminishing roles, while the role of the chemical reaction resistance increases.

Combustion of volatiles produces a characteristic peak at the beginning of the carbon dioxide and oxygen traces. The oxygen peak is somewhat greater than the carbon dioxide peak as a result of the oxygen consumption in the formation of other oxides such as NO_x , CO , SO_2 and H_2O during the combustion of volatiles. For larger diameters the volatiles peak is well pronounced, but diminishes in size as the particle diameter decreases. It has been shown (Pillai, 1981) that the time required for volatiles emission increases with increasing particle size (see equation E.3.7). The extent of volatiles combustion, in the fluidized bed used here, is relatively high for big particles, since the volatiles are released at a slower rate and are available for combustion over a longer period of time. The absence of a volatiles peak on the traces for smaller diameter particles is thought to be the result of the limited residence time of volatiles due to their rapid release. Furthermore, it is true to say that a shorter time is required to char the coal due to the smaller particle diameters, which results in the char and volatile combustion contributions to coincide.

6.2 THE MATHEMATICAL DESCRIPTION OF THE COMBUSTION DATA.

The combustion models, previously mentioned in section 3.0 (i.e. the shrinking core and shrinking particle models), have several unknown parameters, namely, the Sherwood number (Sh), the ash layer diffusion coefficient (D_a), the surface reaction rate constant (K_s) and the parameter X . The parameter X , commonly referred to as the 'cross-flow factor', represents the number of times a bubble is flushed through the system. The evaluation of these parameters, using the experimentally derived data, is discussed below in detail.

6.2.1 ANALYSIS OF TAVISTOCK DUFF COAL

The burnout time data at 715 °C and 848 °C was analysed using program MOD (see section 4.2). The regression results are summarized in tables 6.1-6.3. The evaluated model parameters were substituted into program TRACE to produce the predictions of the carbon dioxide traces for various particle diameters and sample masses. The theoretical and experimental traces are depicted in figures 6.16-6.23.

The values used in the devolatilization time expression, i.e. $\tau_D = D_p^2$ were obtained from the research work of Pillai (1981), who experimentally determined the devolatilization times of various coals in a fluidized bed. Pillai found that τ_D was strongly dependant on the coal particle's initial diameter, the coal type and the bed temperature and that it depended weakly on the mass of the coal sample charged. The values of $a=18$ and $u=0.5$ represent the devolatilization process at 775 °C of Glen Brook coal, which is a bituminous Ohio coal. This temperature is conveniently near the median of 715 °C and 848 °C. The Glen Brook coal values were chosen because its proximate analysis resembles closely the analysis for Tavistock duff coal.

Table 6.1 Linear regression of T_b versus M_c plots for
Tau/stock duff coal at 715 °C.

Gas velocity m/s	Particle diameter D_p mm	Slope s/g	Y-axis intersect s	Cross flow factor X	Sherwood number Sh $T_U=8 \quad T_U=180 \text{ } ^\circ\text{C}$
0.1901	1.09	51.26	102.33	1.485	.225 .275
	2.18	68.8	176.86	0.675	.522 .615
	3.08	69.38	269.21	0.361	.682 .773
	4.5	75.8	452.14	0.211	.867 .947
0.2329	1.09	44.37	109.61	1.284	.210 .253
	2.18	51.35	214.56	0.753	.429 .489
	2.58	47.66	265.83	0.979	.485 .544
	3.08	64.78	326.83	0.319	.562 .622
	4.5	62.74	481.73	0.363	.814 .884

The parameters X and Sh in table 6.1 (calculated from the simple linear regression of the data, see slope and Y-axis intercept) display definite trends with regards to the particle diameter i.e. as the diameter increases, so does the Sherwood number, while the parameter X decreases. Although the Sherwood values are not necessarily representative of the combustion process, they do follow the same trend as indicated by the Ranz & Marshall (1952) Sherwood correlation. Smaller values of parameter X indicate a relatively poor convective mass transfer process, which would cause the char combustion process to become controlled to a greater extent by this particular process. The research work of Chakraborty (1981) suggests that the forced convective mass transfer resistance becomes an increasingly important factor in the combustion process as the particle size increases. This suggestion is reflected in the variation of X with D_p in table 6.1 However one must bear in mind that Chakraborty's experiments were carried out in a shallow fluidized bed where the carbon loading was much higher than in the experiments performed in this investigation.

The three basic forms of the shrinking particle combustion model (see section 3.3.1) were used to describe the combustion data at 715 °C. The parameters obtained from the regression analysis are listed in table 6.2. The film diffusion and kinetic (constant Sh) form of the shrinking particle model was used in the analysis of the data for the experiments at 848 °C. The regression results are listed in table 6.3. Allowance for a devolatilization time is indicated by an appropriate value in the ' τ_v ' column. The Sh and k_c parameters listed in tables 6.2 and 6.3 were evaluated using equation E.3.21 ($b=2$) and equation E.3.22, respectively. (cf. section 3.3.1).

Table 6.2 Regression results for combustion of Tavistock Duff coal at 715 °C.

Model Description	τ_v s	Cross flow factor X	Sherwood number Sh	Surface reaction rate constant k_c m/s
Film Diffusion Avedesian & Davidson, (1973).	180 J s 0.0	0.3 0.2	0.972 0.857	--- ---
Film Diffusion and kinetic (constant Sh)	180 J s 0.0	0.75 0.755	2.831 3.863	0.2437 0.19
Film Diffusion and kinetic (variable Sh)	180 J s 0.0	0.5349 0.4774	--- ---	0.4212 0.3329

Table 6.3 Regression results for combustion of Tavistock Duff coal at 840 °C.

Model Description	τ_v s	Cross flow factor X	Sherwood number Sh	Surface reaction rate constant K_c m/s
Film diffusion and kinetic (constant Sh)	180, s 0.0	0.75 0.755	2.578 3.442	.3364 .2504

The plots of T_c versus M_c for both the experimental data and the theoretical models (based on the values given in tables 6.2 and 6.3) are given in figures 6.8 to 6.15. The various devolatilization time assumptions hardly affect the predictions of the burnout time data, since the value of τ_v employed merely shifts the plot up or down and thus maintaining the slope of the original plot. This vertical shift is indicated by the roughly constant X values. However, the prediction of the carbon dioxide trace data is greatly influenced by the value of τ_v used. This is expected since the carbon dioxide traces must represent the same mass of carbon burnt i.e. area under the curve, irrespective of the assumptions used.

Comparing the regression results for the two bed temperature conditions indicates that the surface reaction rate constant increases with temperature, as is expected. The evaluated Sherwood numbers remain roughly constant and are not far from the theoretical minimum value of 2.

The predictions of the carbon dioxide trace using the three forms of the shrinking particle combustion model, as listed in table 6.2, are compared in figure 6.16 for $\tau_v=180$ s and in figure 6.17 for $\tau_v=0$. Allowing for a small devolatilization time in the analysis of the char combustion

process results in a remarkably better representation of the carbon dioxide trace. Comparing figures 6.16 and 6.17 one observes that the prediction of the burnout time is not affected much by the value of T_0 used. However in all three models the initial carbon dioxide concentrations are grossly underestimated for $T_0=0$. It is felt that the above observations provide convincing evidence that there exists a small initial time period during which volatile emission and the "establishment of char combustion" takes place.

It appears from figure 6.10 that the film diffusion and kinetic (constant Sherwood number) form of the shrinking particle model represents best the experimental data. This model not only predicts the burnout time, but also predicts the maximum carbon dioxide concentration and the general shape of the trace fairly well. The film diffusion model underestimates the maximum carbon dioxide concentration and predicts a very sharp decline in the carbon dioxide concentration near the burnout time, which is quite obviously not the case. The variable Sherwood expression represents the data moderately well. The reason for this is the possible over estimation of the film diffusion term. The Sherwood number in this term is given by the Ranz & Marshall correlation. By the nature of the experimental conditions, i.e. relatively small gas velocities, the Sherwood correlation would yield Sh values close to 2. The smaller Sh numbers result in an over estimation of the role of the film diffusion resistance. The consequent underestimation of the kinetic resistance results in a "flatter" shaped carbon dioxide trace, as can be seen from figure 6.16. The decreased role of the kinetic resistance is portrayed by the relatively high reaction rate coefficient values listed in table 6.2 for the variable Sherwood model.

In the following theoretical predictions the film diffusion and kinetic (constant Sh number) expression was used allowing for a devolatilization time.

The prediction of the experimental carbon dioxide traces for

a range of particle diameters, gas velocities and sample masses are depicted in figures 6.18-6.23. The selected model is capable of satisfactorily predicting the combustion behaviour of Tavistock duff coal over the range of experimental conditions employed.

Ross & Davidson (1981) conducted an investigation into the combustion of carbon particles at 1173 K in a fluidized bed and concluded that the following was the surface reaction :



The rate constant for this reaction is given by Field (1967) as

$$K_C = 595000 T_p \exp(-149227/R_g T_p) \quad \text{----- (E.6.2)}$$

where :

K_C - surface reaction rate constant

T_p - particle surface temperature

R_g - universal gas constant

The experimentally derived K_C values are compared with equation (E.6.2) in figure 6.24. At first glance one observes that the K_C data points deviate considerably from equation (E.6.2), although they do follow the same trend. However one must realize that the particle surface temperature is not necessarily the bed temperature. In fact it has been shown by various researchers, Yates & Walker (1978), Ross, Patel & Davidson (1981), Chakraborty & Howard (1979), using photography and thermocouples imbedded in burning char particles, that the particle temperature can exceed the bed temperature by 150 K. Accounting for this temperature deviation, the experimentally derived K_C values are in better agreement with the K_C values predicted from equation (E.6.2). From figure 6.24 one may note that extrapolation of the data from this investigation to 1173 K, would yield a K_C value close to that obtained by Ross & Davidson (1981).

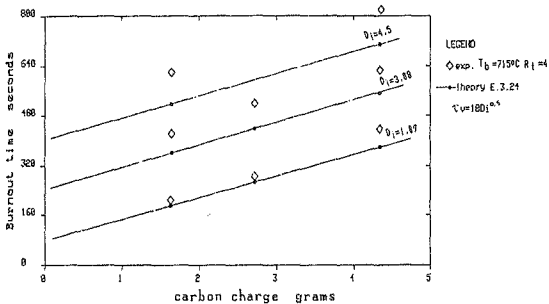


Figure 6.8 Tavistock burnout time versus mass of carbon charge

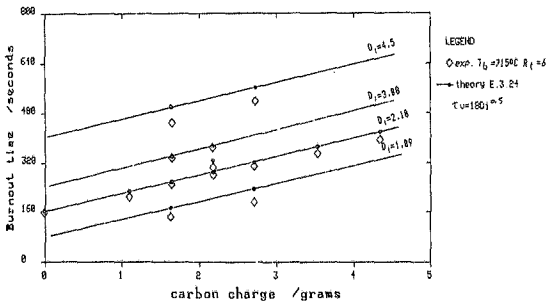


Figure 6.9 Tavistock burnout time versus mass of carbon charge

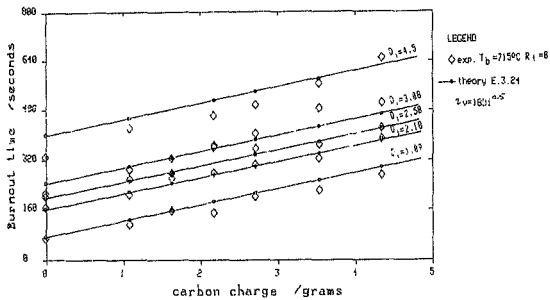


Figure 6.10 Tavistock burnout time versus mass of carbon charge

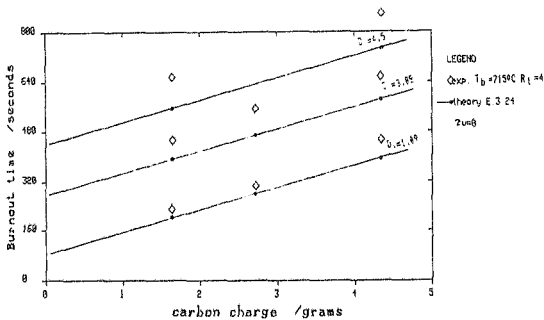


Figure 6.11 Tavistock burnout time versus mass of carbon charge

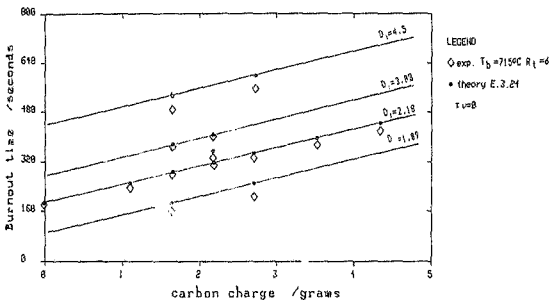


Figure 6.12 Tavistock burnout time versus mass of carbon charge

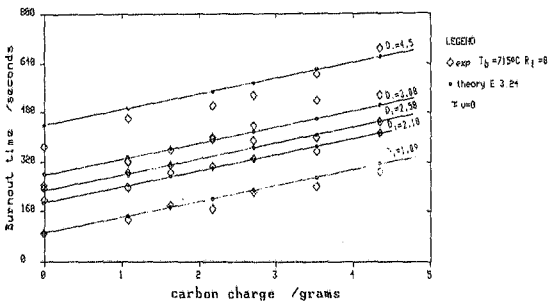


Figure 6.13 Tavistock burnout time versus mass of carbon charge

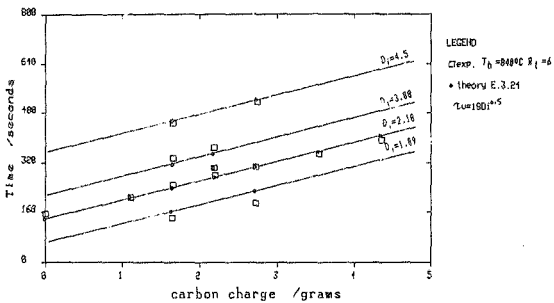


Figure 6.14 Tavistock burnout time versus mass of carbon charge

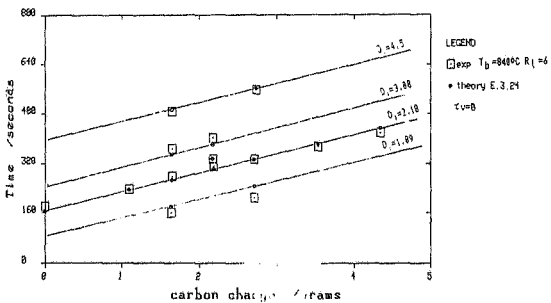


Figure 6.15 Tavistock burnout time versus mass of carbon charge

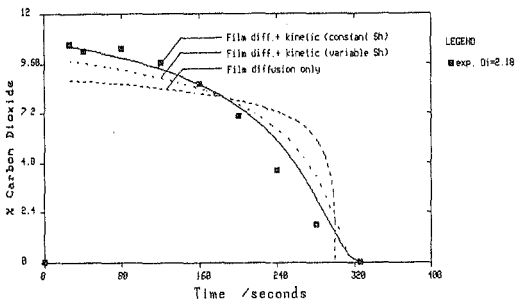


Figure 6.16 Comparison of model predictions $\nu=100$ $T_b=715^\circ\text{C}$

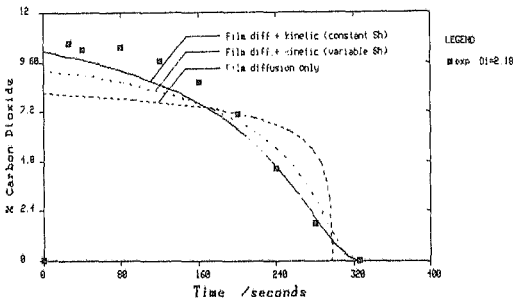


Figure 6.17 Comparison of model predictions $\nu=0$ $T_b=715^\circ\text{C}$

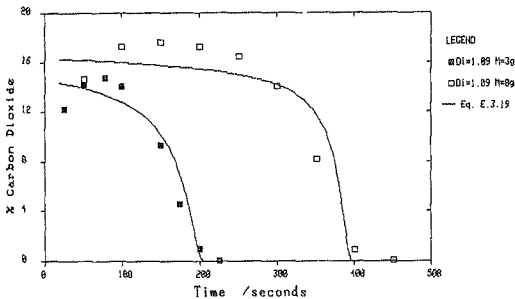


Figure 6.18 CO2 trace prediction $T=715^{\circ}\text{C}$ $Rt=4$ $Di=1.09$

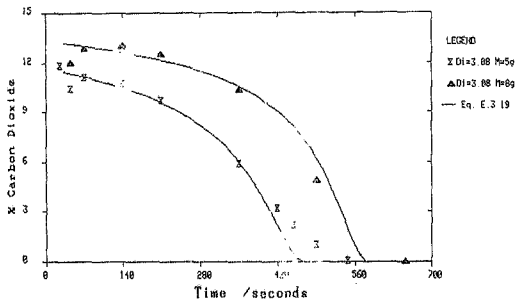


Figure 6.19 Tavistock CO2 trace prediction $T=715^{\circ}\text{C}$ $Rt=4$ $Di=3.08$

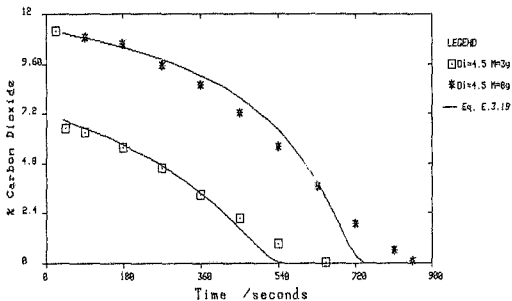


Figure 6.20 Tavistock CO₂ trace prediction $T_h=715^{\circ}C$ $R_t=4$ $Di=4.5$

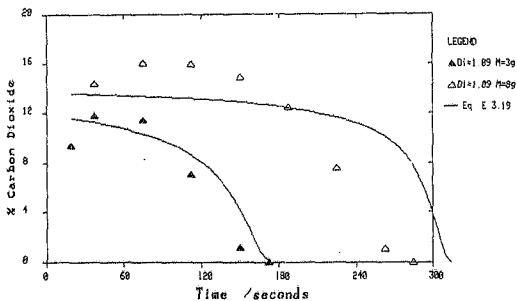


Figure 6.21 Tavistock CO₂ trace prediction $T_h=715^{\circ}C$ $R_t=8$ $Di=1.09$

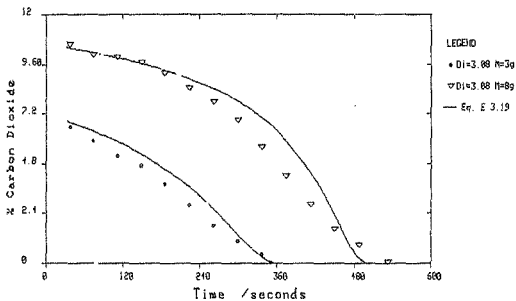


Figure 6.22 Tavistock CO2 trace prediction $T_b=715^{\circ}\text{C}$ $Rt=8$ $D1=3.08$

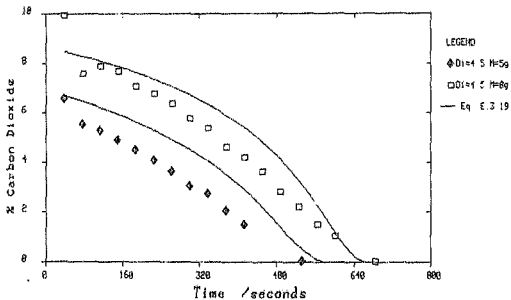


Figure 6.23 Tavistock CO2 trace prediction $T_b=715^{\circ}\text{C}$ $Rt=8$ $D1=1.5$

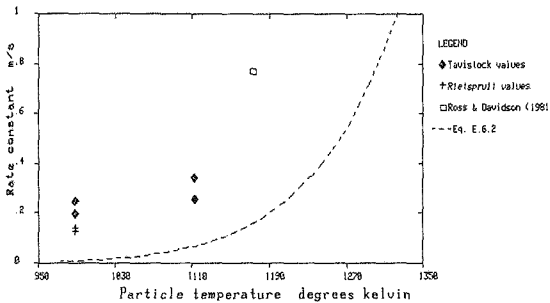


Figure 6.24 Rate constant versus particle surface temperature

6.2.2 ANALYSIS OF RIETSPRUIT DISCARD COAL

The regression results obtained from program MDD, using the theory developed in section 3.3.2, for the Rietspruit discard burnout time data are listed in table 6.4.

Table 6.4 Regression results for Rietspruit Discard at 7150C.

Model description	τ_D s	Cross flow factor X	Ash layer diffusion coeff. D_e m ² /s	Sherwood number Sh	Chemical reaction coeff. K_c m/s
Shrinking core	90, .32	0.26	1.1212	---	.1295
ash layer diff.	90, .32	0.06	0.5755	---	.2437†
and reaction model	0.0	0.225	1.2725	---	.1186
Shrinking particle	90, .32	0.26	--	1.8471	.1295
film diffusion and	90, .32	0.06	--	0.9482	.2437†
reaction model					

†-value from Tavistock analysis.

The values used in the devolatilization time (τ_D) expression are $a=9$ and $u=0.32$, which represent the devolatilization figures for Arigna coal, as determined by Pillai (1981). This particular coal is an Irish high-ash content coal and its proximate analysis resembles closely that of Rietspruit Discard.

The surface reaction rate constant obtained from the regression of Tavistock data was used in the description of Rietspruit coal data, since it was felt that the value of K_c obtained from the straight forward regression of the Discard data was underestimated. This underestimation resulted in the role of ash layer diffusion term to become

less important and hence to produce carbon dioxide traces with less pronounced concave shapes. The use of the K_c value for Tavistock coal, should not be seen as implying that the two coals possess similar combustion quantities in relation to the chemical reaction resistance. However, it would be reasonable to assume that the two carbon types exhibit the same surface reaction and thus the use of Tavistock's rate constant is justified. The prediction of the burnout time data is little affected by the choice of K_c or X from the values in table 6.4, as can be seen from the comparison plot in figure 6.26.

The shrinking core (ash layer and kinetic) model predictions of the carbon dioxide trace, using the two K_c values, are given in figure 6.26. Quite clearly a better representation of the data is obtained by increasing the relative role of the ash layer diffusion resistance. Furthermore the shrinking particle model prediction of the carbon dioxide trace fails to represent the data since the theoretical curve is convex while the experimental is concave. It is interesting to note that the shrinking core and shrinking particle models represent the burnout time data with the same degree of accuracy. This is due to the fact that the form of the burnout time expression (equation E.3.24) in both instances is the same. Thus the Sherwood number in table 6.4 was obtained by equating equations (E.3.21) in section 3.3.1 and equation (E.3.36) in section 3.3.2, which yields the following expression: $Sh=288 De/(96 Dg)$.

The shrinking core model, allowing for a greater ash layer diffusion resistance, was used in all the subsequent predictions and comparisons.

Figures 6.27 and 6.28 represent the carbon dioxide trace for Rietspruit Discard particles of diameters 4.5 and 3.08 mm, respectively. The theoretical model represents the data fairly well. However the deviation between reality and the theory increases with the increasing mass of carbon charge. It is felt that this increasing deviation is as a result of the hydrodynamic term, viz. C_0 , been overestimated i.e.

parameter X is too small. Figure 6.28 shows the flue gas oxygen concentration versus a dimensionless rate coefficient (K') and is parameterized by the cross flow (hydrodynamic) factor X . From figure 6.28 one notes that the combustion process becomes particularly sensitive to the hydrodynamic factors of the reactor when K' is large. The dimensionless rate coefficient is proportional to the mass of carbon charge (cf. equations E.3.16 and E.3.33) and thus the prediction of the combustion behaviour of the coal sample for relatively large carbon charges is strongly dependant on the description of the reactor hydrodynamics. It is plausible to assume that the coal type would not effect the reactor hydrodynamics and thus the parameter X evaluated from Rietspruit data will be similar to the value obtained from the analysis of Tavistock data (instead of being 3 times smaller). An increased X value would in essence increase the relative role of the ash layer diffusion term and predictions of the combustion process at larger carbon masses would become more representative.

One should note that the experimental burnout time data for Rietspruit coal is more scattered than for the Tavistock data. This scatter may be attributed to the extremely non-homogenous nature of the discard coal which results in a fairly high deviation in the fixed carbon analysis over a range of samples. It is understandable if one is hesitant to accept the regression results of the Rietspruit Discard coal as being meaningful. However, one must bear in mind that the data not only displays consistent trends, but also provides definite proof that the ash layer diffusion resistance plays a dominant role in controlling the overall combustion process. It is agreed that the regression of the data is deficient in predicting the parameters accurately. However, subsequent logical modification of these parameters has provided representative predictions of the Rietspruit discard carbon dioxide traces.

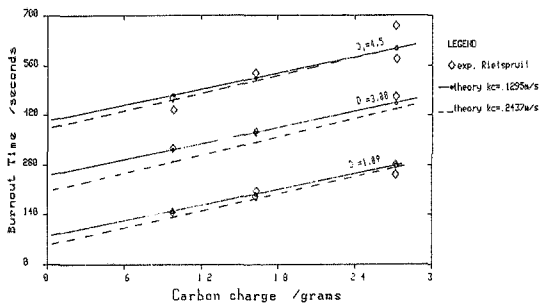


Figure 6.25 Burnout line versus mass of carbon charge $T_b=715$ C $Rt=6$ $\tau_v=9D^{0.52}$

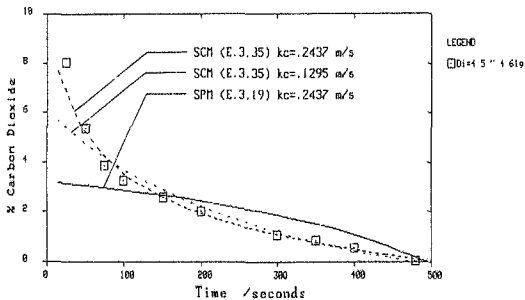


Figure 6.26 Comparison of Rietspruit CO2 trace predictions $T_b=715$ C $\tau_v=9D^{0.52}$

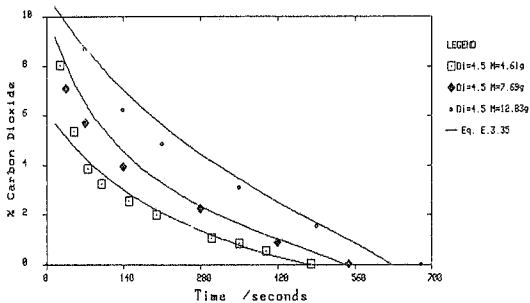


Figure 6.27 Rietspruit CO₂ trace prediction Tb=715°C Rt=6 Di=4.5

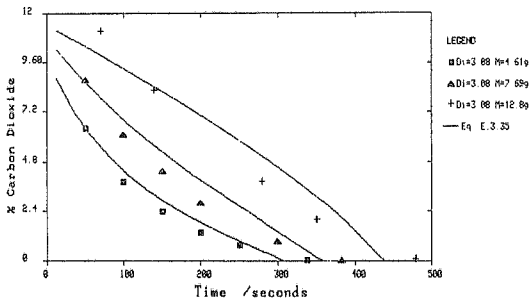


Figure 6.28 Rietspruit CO₂ trace predictions Tb=715°C Rt=6 Di=3.08

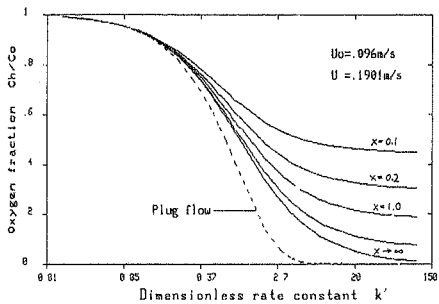


Figure 6.29 Oxygen fraction versus dimensionless rate constant

7. EVALUATION OF THEORETICAL APPROACH.

In agreement with the opinions generally expressed in the literature this investigation has shown that the char combustion process is controlled by a combination of the film diffusional and chemical reaction resistances. In the case of the high ash content discard coal, the char combustion process has been shown to be strongly influenced by the ash layer diffusion resistance. The results of the combustion data analysis strongly suggest that the coal combustion process is broadly divided into two distinct phases, viz. an initial devolatilization and "establishment of combustion" period, which is followed by the combustion of the residual char. The magnitude of this initial period for Tavistock and Rietspruit coals was not quantitatively established. However the incorporation of suitable T_0 times provided an enhanced description of the combustion data.

It is believed that the combustion of Tavistock char, in the temperature range investigated, is strongly influenced by the conditions prevailing at the surface of the char particle. For this reason the char surface reaction during the combustion of Tavistock coal is considered in detail below.

An important factor in determining the rate of reaction at the char surface and consequently the role of the kinetic resistance, is the particle surface temperature. Ross & Davidson (1981) visually observed that large char particles ($> 0.5\text{mm}$) glowed brighter than the surrounding inert bed material, while small char particles ($< 0.5\text{mm}$) were found to be indistinguishable from the bed material. Their data analysis showed that the small particles burned much slower than the large particles and that the value of K_c obtained for small particles was much less than the value obtained for large particles. They suggested that a different mechanism of combustion existed between large and

small particles. For large particles the CO burnt close to the char surface, while for small particles the CO burnt somewhat further from the surface. Consequently, for small particles, the "energy generated" by CO combustion was dissipated by the bed material instead of raising the particle temperature. This difference in the combustion mechanism results in the small particles having a temperature close to the bed temperature, while large particles exhibit a temperature of up to 150 K above the bed temperature. The experimental technique employed in this investigation did not include the measurement of the char particles' surface temperature. However the analysis of the K_C values obtained showed that the particles were indeed hotter than the bed material and that a deviation of 150 K was probable. The significance of the above discussion, is that it is felt that the combustion process of the 1.09 mm particles is different from that of the larger size particles. Comparing the carbon dioxide traces in figures 6.18-6.20, one notes that the theory predicts the shape of the traces fairly well with the exception of the 1.09mm particles. In fact for 1.09mm particles the theoretical curves display the distinct characteristics of a strong film diffusion resistance being present i.e. a "flat" trace having a sharp decline near the burnout time. Quite obviously the contrary situation should prevail i.e. a relatively strong kinetic resistance. This observation suggests that the rate constant, evaluated using all the data at 715 °C, is not representative for all the particle sizes employed. In fact the value of $K_C = 2437$ m/s probably underestimates the value of K_C applicable to the smaller particle size of 1.09mm. A smaller K_C value would result in a greater kinetic resistance and would consequently yield a theoretical trace having a greater curvature than the trace in figure 6.19. In essence this implies that the small particles (1.09mm) exhibit a greater kinetic resistance to combustion than the larger particles. This deviation is probably as a result of the smaller particles having a cooler char surface than the large particles, which is in accordance with the observations of Ross & Davidson (1981).

In section 6 it has been shown that the general form of the shrinking particle (constant Sh number) model, incorporating both film diffusion and kinetic resistances, represents the combustion behaviour of the Tavistock char (cf. equation E.3.19). Furthermore it was shown that the value of $K_c = 0.2437$ m/s was physically acceptable (cf. figure 6.24.) and thus the oxidation of carbon to carbon monoxide is a feasible surface reaction.

As mentioned in section 3.3.1 the parameter b defines two possible reaction mechanisms. The values of the Sherwood number and the surface reaction rate constant, calculated for each mechanism, are listed below in table 7.1.

Table 7.1 The Sherwood number and rate constant values evaluated for Tavistock coal at 715 °C and with $V_g = 1.80$ p.s.

	Mechanism 1 (b=1)	Mechanism 2 (b=2)
Sherwood number	5.702	2.851
Reaction rate constant (m/s)	0.2437	0.2437

In essence mechanism 1 and mechanism 2 represent the same surface reaction, namely:



The difference between these two mechanisms arises from the assumption regarding the rate of the gas phase oxidation of CO i.e.



For mechanism 1 the gas phase reaction (b) is assumed to proceed rapidly, while for mechanism 2 this reaction is assumed to proceed relatively slowly. Thus for mechanism 1 the CO is consumed very close to the surface of the char particle, while for mechanism 2 the CO is consumed in the region surrounding the burning char particles.

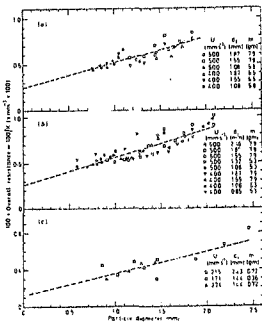


Figure 7.1 Dependence of overall resistance to combustion on particle size. Ross & Davidson (1981).

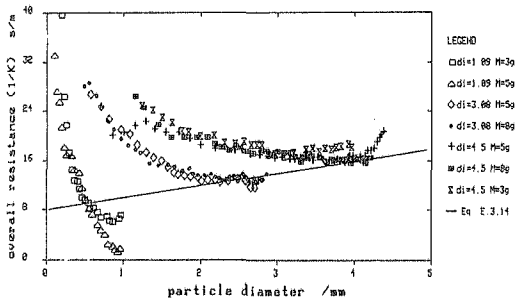


Figure 7.2 Overall combustion resistance versus particle diameter

In order to establish which mechanism is relevant one has to consider the position of the CO combustion relative to the char particle surface. Ross & Davidson found that a linear relationship existed between the overall combustion resistance ($1/K$) and the particle diameter D (cf. equation E.3.14 in section 3.3.1). This relationship implies a constant surface reaction rate constant and hence a constant particle surface temperature, which suggests that in their investigation the CO burnt close to the surface of the char particles. Based on these observations they concluded that mechanism 1 was relevant. Plots of the overall combustion resistance versus particle diameter for the experimental data of Ross & Davidson and for the combustion of Tavistock are presented in figures 7.1 and 7.2, respectively. The data in figure 7.1 were obtained by integrating the carbon dioxide trace over a narrow concentration range. This was done to ensure that the particle temperature remained constant, since Ross, Patel & Davidson (1981) have shown that the particle temperature increases linearly with an increasing oxygen concentration. The data in figure 7.2 was obtained by integrating the whole carbon dioxide trace. The points on figure 7.2, represent three initial particle size ranges. As is expected the 4.5mm and 3.08mm particles follow much the same trends, with the 3.08mm particles exhibiting a smaller combustion resistance. However the 1.09mm particles behave in a distinctly different manner, as they experience a relatively low resistance at the onset of combustion and there after the resistance increases rather sharply as the char combustion proceeds. It is clear from figure 7.2 that $1/K$ is not linear with D throughout the duration of the char combustion process and furthermore $1/K$ does not monotonically increase with increasing diameter, as is indicated by equation E.3.14. The solid line in figure 7.2 represents equation E.3.14 evaluated using the values of Sh and K_G obtained from the regression of the burnout time data. If the integration was performed over a narrow carbon dioxide concentration range (ie. over a flat segment of the trace, which typically exists at the onset of combustion), the solid line would represent the data fairly

well. It is felt that the overall non-linearity, exhibited in figure 7.2, suggests that surface reaction rate constant and the particle surface temperature do not remain constant throughout the combustion process.

At the onset of combustion, of say a large char particle, the CO oxidation occurs close to the char surface and the char surface temperature is higher than the bed temperature. The existence of this high temperature is a result of the proximity of the CO oxidation reaction which ensures that a large proportion of the CO "reaction energy" is available for raising and maintaining the particle surface temperature. However, as the combustion proceeds and the char particle diameter decreases, the CO oxidation moves further away from the char surface. This results in a greater proportion of the CO oxidation "reaction energy" to be dissipated by the inert bed material and a decrease in the ability of the particle to maintain its high surface temperature. It is probable to postulate that a stage is reached where the rate of the combustion reaction is unable to satisfy the energy requirements of the inert material. This temperature decrease would cause the surface reaction rate constant to decrease. The overall resistance ($1/K$) would thus not vary linearly with the particle diameter (D), since the value of the reaction rate constant (k_c), in essence, varies with the particle diameter. The ideas postulated above are consistent with the curves presented in figure 7.2 and they are acceptable explanations for the observed combustion behaviour. It has been previously suggested (Ross & Davidson, 1981) that small particles in comparison to large particles exhibit a different mechanism of combustion. The above discussion suggests that as the large particles burn down to small particles they experience a change in their combustion mechanism due to the location of the CO reaction.

In order to demonstrate the effect of a variation of the k_c value on the carbon dioxide trace a brief numerical experiment was conducted. For simplicity the surface reaction rate constant was assumed to vary linearly

with the particle diameter viz:

$$K_c(D) = \frac{F \bar{k}_c}{D_i} D + \bar{k}_c (1-F) \quad \text{----- (E.7.1)}$$

where :

F is a variation factor, for positive F values the particle temperature decreases with time while for negative values the particle temperature increases with time.

\bar{k}_c is the surface reaction rate constant at the onset of combustion and was equated to the value obtained from the regression analysis, i.e. 0.2437 m/s

The chemical reaction resistance term in equation E.3.19 of section 3.3.1 was accordingly modified to yield the following term: (see appendix C)

$$\text{chemical resistance term} = \frac{v_c D_i}{24 C_o F \bar{k}_c} \ln \frac{F \bar{k}_c / D_i + \bar{k}_c (1-F) / D_i}{F \bar{k}_c x / D_i + \bar{k}_c (1-F) / D_i}$$

The effect of incorporating equation (E.7.1) into the combustion analysis is portrayed in figure 7.3. A remarkably better representation of the experimental data is obtained by assuming that the surface reaction rate constant decreases with time viz. $F=+0.5$ on figure 7.3.

One observes, from table 7.1, that the Sh number applicable to mechanism 1 is twice the Sh number obtained for mechanism 2. Pillai (1981) and Jung & Stangmore, (1980) obtained values of the Sh number in the region of 4-6. However, as pointed out by these researchers, the high Sh numbers obtained were as a result of their experimental conditions viz. gas velocities in excess of 1m/s and particle diameters of up to 10mm. The gas velocities and particle diameters employed in this investigation were in the region of 0.2m/s and 4.5mm, respectively. Under these somewhat mild conditions one would expect the Sh numbers to be relatively close to 2. Thus it is felt that the Sh number of 5.702, as obtained for mechanism 1, is unrealistic with

regards to the experimental conditions of this investigation.

In view of the above discussion, it is felt that the char particles do not experience a constant surface temperature. This variation is probably caused by the CO reaction having a relatively slow rate of reaction and consequently the location of the CO combustion reaction is not confined to a region close to the char particle surface. Thus mechanism 2 is relevant to the combustion of Tavistock coal under the operating conditions employed in this investigation.

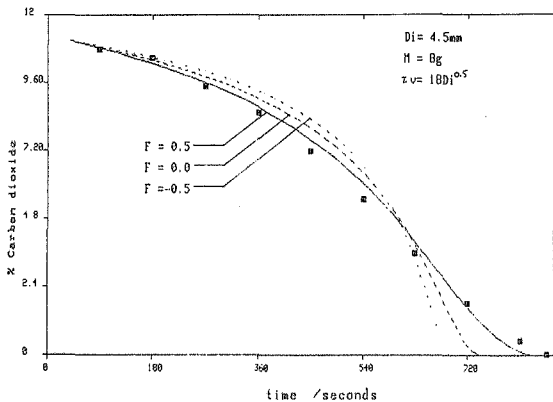


Figure 7.3 Prediction of carbon dioxide trace Tb=715 °C Rt=4.

8. CONCLUSION

This investigation was primarily concerned with the analysis of the combustion behaviour of Tavistock Duff and Rietspruit Discard coals at 715 °C. Analysis of the experimental data has clearly shown the following :

- the high ash content Rietspruit char combusts in a shrinking core mode and the overall combustion resistance is a combination of the ash layer diffusional resistance and the kinetic resistance.
- the combustion of Tavistock char is represented by the shrinking particle mode of reaction and the overall combustion resistance is the summation of the film diffusional and kinetic resistances.
- the char surface reaction is the oxidation of carbon to carbon monoxide.
- the rate of the gas phase carbon monoxide reaction is relatively slow, which results in the location of this reaction to exist at a point removed from the char surface.
- the char particle surface temperature presumably decreases with time and particle diameter.
- the burnout time of a coal sample is the summation of the devolatilization time and the char burnout time.

In the initial theoretical consideration the reaction rate constant k_c was regarded as a constant with respect to time. From the results of this investigation it appears that the rate constant varies during the char combustion process, due to the variation of the surface temperature. However the combustion models and their associated evaluated parameters do represent all aspects of the combustion process over a fair period of time after the onset of combustion. The gas concentrations during this period of time are representative of those concentrations found in practical fluidized bed combustion systems. Furthermore, the combustion models do represent the particle burnout times with acceptable accuracy. The maximum theoretical deviations from reality

occur under conditions which are not experienced during the normal operation of practical combustors and thus the combustion models obtained from this investigation are of importance to the understanding of these practical combustors.

... ..

occur under conditions which are not experienced during the normal operation of practical combustors and thus the combustion models obtained from this investigation are of importance to the understanding of these practical combustors.

9. REFERENCES

- Arthur, J.R., Reaction between carbon and oxygen, 1951, Trans. Faraday Soc., 47, 164.
- Avedesian, M.M. & Davidson, J.F., Combustion of carbon particles in a fluidised bed, 1973, Trans. IChemE, 51:121
- Basu, P., Broughton, J. & Elliott, D.E., Combustion of single coal particles in fluidised beds, 1975, Proc. Inst. Fuel Sym Series No. 1: Fluidized Combustion, A3-1.
- Campbell, E.K. & Davidson, J.F., The combustion of coal in fluidised beds, 1975, Proc. Inst. Fuel Sym. Series No. 1: Fluidized Combustion, A2-1.
- Chakraborty, R.K. & Howard, J.R., Burning rates and temperatures of carbon particles in a shallow fluidised-bed combustor, 1978, J Inst Fuel, 51, 220-224
- Chakraborty, R.K. & Howard, J.R., Combustion of char in shallow fluidised bed combustors: influence of some design and operating parameters, 1981, J Inst Energy, 48-54.
- Chen, T.P. & Saxena, S., Mathematical modelling of coal combustion in fluidised beds with sulfur emission control by limestone or dolomite, 1977, Fuel, 56, 401.
- Davidson, J.F. & Harrison, D., 1963, Fluidized Particles, Cambridge: The University Press.
- Field, M.A., Gill, D.W., Morgan, B.B. & Hawksley, P.G.W., 1967, Combustion of Pulverised Fuel, BCURA.
- Gibbs, B.M., A mechanistic model for predicting the performance of a fluidised bed coal combustor, 1975, Proc. Inst. Fuel Sym. Series No. 1: Fluidised combustion, A5-1.

- Golovina, E.S. & Khaustovich, G.P., Eight Symposium (International) on Combustion, 1962, 784, The Combustion Institute.
- Hougen, O.A. & Watson, K.M., Chemical Process Principles Part 3, Kinetics and Catalysis, 1947, John Wiley & Sons, New York.
- Jung, K. & Stangmore, B.R., Fluidised bed combustion of wet brown coal, 1980, Fuel, 59, 74-80.
- Levenspiel, O., Chemical reaction engineering, 1972, John Wiley & Sons, New York.
- Patel, M.S., 1979, PhD Dissertation, (University of Cambridge).
- Pillai, K.K., The influence of coal type on devolatilization and combustion in fluidized beds, 1981, J Inst Energy, 142-158.
- Ranz, W.E. & Marshall, W.R. Jr., Evaporation from drops, 1952, Chem Eng Progr, 48:141.
- Ross, I.B. & Davidson, J.F., The combustion of carbon particles in a fluidised bed, 1981, Trans IChemE, 59:108-114.
- Ross, I.B., Patel, M.S. & Davidson, J.F., The temperature of burning carbon particles in fluidised beds, 1981, Trans IChemE, 59:83-88.
- Saxena, S.C. & Turek, D.G., Development of a simple fluidised-bed combustion model for the assessment of a pressurized fluidized-bed combustion system for electrical power generation., 1980, DOE/METC/SP-80/15, NTIS publication.
- Strehlow, R.A., 1968, Fundamentals of combustion, International Textbook Company.
- Tomeczek, J., Communication, 1979, Trans IChemE, 57:215.
- Yates, J.G., Fundamentals of fluidized-bed chemical processes, 1983, Butterworths monographs in chemical engineering.

Appendix A.

- Tavistock Duff burnout time data
- Rietspruit Discard burnout time data

Tavistock Duff burnout time data.

Bed temperature : 528 °C fluidising velocity : 0.2626 m/s

Particle diameter /mm	Sample mass /g	Burnout time /s
1.09	3.02	386.25
2.18	3.00	472.50
2.58	3.02	540.00
3.08	5.00	547.50
4.58	3.01	652.50

Bed temperature : 840 °C fluidising velocity : 0.2141 m/s

Particle diameter /mm	Sample mass /g	Burnout time /s
2.18	0.00	170.00
2.18	2.03	232.50
2.18	3.03	273.75
2.18	4.03	309.75
2.18	5.00	330.00
2.18	6.51	371.25
2.18	8.00	416.25
1.09	5.00	206.25
1.09	3.02	157.50
2.58	4.00	330.00
3.08	3.03	363.75
3.08	4.00	397.50
4.58	5.04	551.25
4.58	3.03	483.75

Bed temperature : 715 °C fluidising velocity : 0.1473 m/s

Particle diameter /mm	Sample mass /g	Burnout time /s
3.08	3.03	450.00
3.08	5.02	547.50
3.08	8.00	652.50
1.09	3.02	225.00
1.09	8.00	450.00
1.09	5.01	300.00
4.58	3.04	652.50
4.58	8.01	855.00

Bed temperature : 715 °C fluidising velocity : 0.1981 m/s

Particle diameter /mm	Sample mass /g	Burnout time /s
1.09	5.00	248.00
1.09	3.02	187.50
2.18	2.03	236.25
2.18	3.03	285.00
2.18	4.03	307.50
2.18	5.00	341.25
2.18	6.51	390.00
2.18	8.00	420.00
3.08	3.03	382.50
3.08	4.00	431.50
3.08	5.00	510.00
4.50	5.04	654.25
4.50	3.03	573.75

Bed temperature : 715 °C fluidising velocity : 0.2329 m/s

Particle diameter /mm	Sample mass /g	Burnout time /s
1.09	0.00	82.61
1.09	2.00	127.50
1.09	3.00	172.50
1.09	4.00	165.00
1.09	5.00	217.50
1.09	6.50	236.50
1.09	8.00	285.00
2.18	0.00	189.50
2.18	2.00	232.50
2.18	3.00	281.25
2.18	4.00	300.00
2.18	5.00	326.25
2.18	6.50	348.75
2.18	8.00	408.75
2.50	0.00	228.09
2.50	2.00	281.25
2.50	3.00	303.75
2.50	5.00	382.50
2.50	6.50	393.75
2.50	8.00	446.25
3.08	0.00	239.38
3.08	2.00	315.00
3.08	2.00	318.75
3.08	3.00	352.50
3.08	4.00	386.25
3.08	4.00	393.75
3.08	5.00	431.25
3.08	6.50	513.75
3.08	8.00	532.50
4.50	0.00	362.01
4.50	2.00	457.50
4.50	4.00	498.75
4.50	5.00	532.50
4.50	6.50	600.00
4.50	8.00	682.50

Rietspruit Discard burnout time data.

Bed temperature : 715 °C fluidising velocity : 0.1981 m/s

Particle diameter /mm	Sample mass /g	Burnout time /s
3.08	7.69	382.58
3.08	12.84	480.08
3.08	4.61	337.58
4.50	12.86	588.75
4.50	4.61	488.08
4.50	7.69	547.58
4.50	12.83	682.58
4.50	4.65	446.25
1.09	7.68	198.75
1.09	12.84	258.75
1.09	7.71	213.75
1.09	12.85	285.88
1.09	4.61	153.75

Appendix B.

- program TRACE
- program MOD

Appendix C.

The kinetic resistance term may be expressed as follows :

$$\int \frac{P_c}{24 C_0 k_c} dd$$

Integration of the above expression, regarding k_c as a constant with respect to the particle diameter, results in the expression for Ω_2 as given in equation E.3.22 of section 3.3.3. However, if k_c is assumed to vary linearly with the particle diameter, for example :

$$k_c(d) = \frac{F \bar{k}_c d}{d_i} + \bar{k}_c (1-F)$$

then the integration yields the following expression for the kinetic resistance term :

$$\frac{P_c d_i}{24 C_0 F \bar{k}_c} \ln \left\{ \frac{F \bar{k}_c / d_i + \bar{k}_c (1-F) / d_i}{F \bar{k}_c \times / d_i + \bar{k}_c (1-F) / d_i} \right\}$$

Appendix D.

The bed material elutriated during the combustion of a coal sample was obtained at the end of the experiment by emptying the cyclone dropout chamber. The elutriated material was weighed and the carbon content was determined analytically. The results obtained for various coal samples are given below in table D.1.

Table D.1 Elutriation data for the combustion of Tavistock Duff coal at 715°C and $U=0.198\text{m/s}$.

Particle diameter mm	Coal sample mass g	Elutriated bed material mass g	Elutriated carbon mass g
4.5	5.00	1.25	0.016
4.5	3.00	0.88	0.006
4.5	10.05	0.67	0.025
1.5	15.12	2.98	0.050
1.5	10.00	1.80	0.010
1.5	3.60	0.91	0.020
1.5	5.07	1.43	0.015
1.09	10.04	1.67	0.021
1.09	5.00	0.65	0.016
1.09	5.00	0.81	0.060

The elutriation data tabulated above indicates that the amounts of carbon elutriated are small in comparison to the amounts of fixed carbon that remained in the fluidized bed.

Appendix E.

A typical bed temperature profile for the combustion of Tavistock Duff coal samples is given in figure E.1.

The temperature controller was capable of maintaining the bed temperature within 5°C of the setpoint temperature.

Figure E.1 indicates that the maximum bed temperature rise experienced during the combustion of Tavistock Duff coal was 15°C.

Similar temperature profiles were obtained for Rietspruit Discard coal, since the amounts of Rietspruit coal charged into the fluidized bed were chosen such that the quantities of fixed carbon were identical to those employed during the experiments using Tavistock coal.

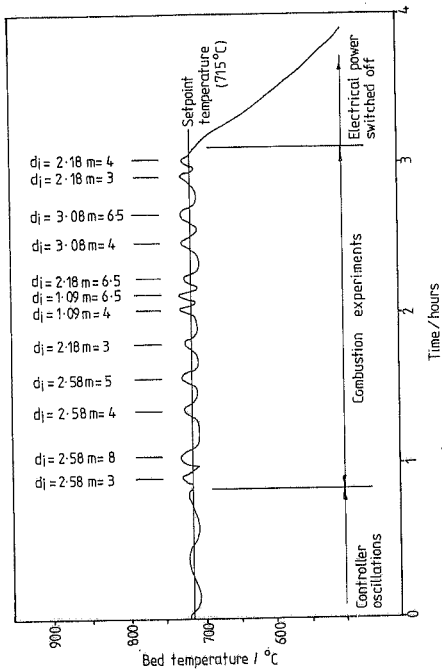


FIGURE E.1 TEMPERATURE PROFILE FOR A TYPICAL SERIES OF TAVISTOCK COMBUSTION TRIALS

Appendix F.

- dimensioned fluidized bed reactor drawings .

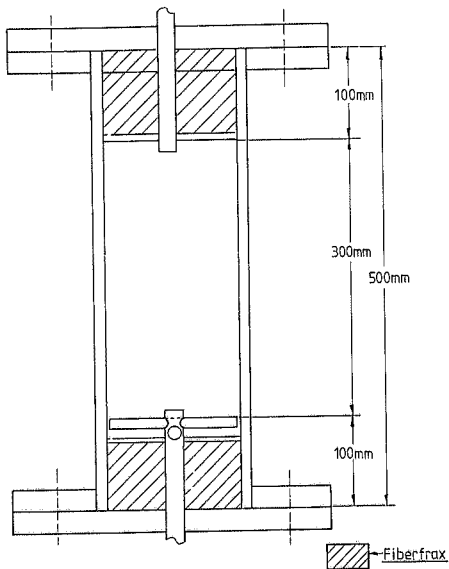


FIGURE F.1 SECTIONED SIDE VIEW OF FLUIDIZED
BED REACTOR

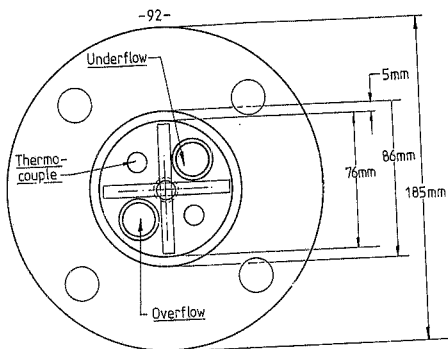


FIGURE F.2 TOP VIEW OF DISTRIBUTOR PLATE

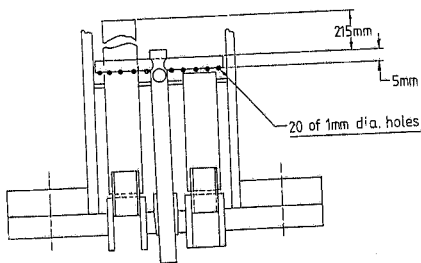
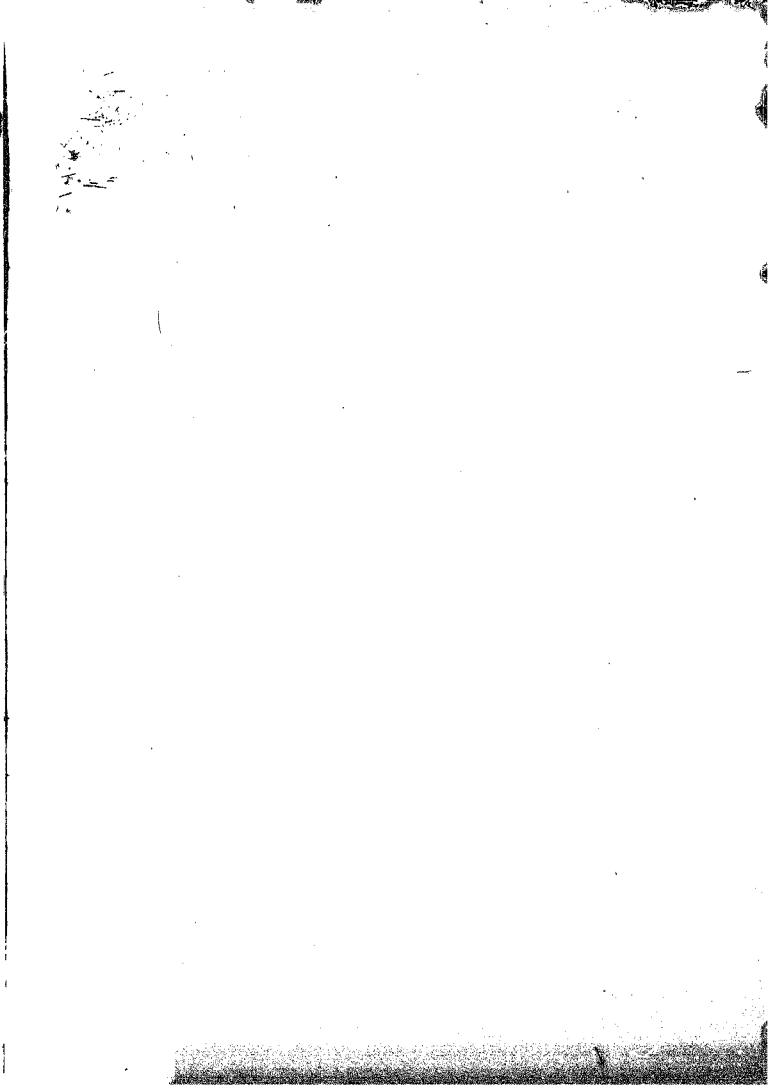


FIGURE F.3 SECTIONED SIDE VIEW OF DISTRIBUTOR PLATE



Author Hamman Andre Pieter

Name of thesis The Fluidised Bed Combustion Characteristics Of Some Inferior Quality South African Coals. 1985

PUBLISHER:

University of the Witwatersrand, Johannesburg

©2013

LEGAL NOTICES:

Copyright Notice: All materials on the University of the Witwatersrand, Johannesburg Library website are protected by South African copyright law and may not be distributed, transmitted, displayed, or otherwise published in any format, without the prior written permission of the copyright owner.

Disclaimer and Terms of Use: Provided that you maintain all copyright and other notices contained therein, you may download material (one machine readable copy and one print copy per page) for your personal and/or educational non-commercial use only.

The University of the Witwatersrand, Johannesburg, is not responsible for any errors or omissions and excludes any and all liability for any errors in or omissions from the information on the Library website.